Recent Developments in Rotary-Wing Aerodynamic Theory

Wayne Johnson
NASA Ames Research Center, Moffett Field, California

Introduction

ROTARY-wing flowfields are as complex as any in aeronautics. The helicopter rotor in forward flight involves three-dimensional, unsteady, transonic, viscous aerodynamic phenomena. Helicopter aerodynamic theory benefited greatly from the introduction of digital computing methods.[1] Rotary-wing problems still provide a stimulus for development and opportunities for application of the most advanced computational techniques.

The present survey examines the progress in development of advanced computational methods for rotary-wing aerodynamics. The mathematical basis for the principle lines of investigation is summarized. With this common background, the recent published work in each area is reviewed. It is the intent that this survey cover not the computational techniques that could be, but rather those that have been applied to rotary-wing aerodynamics. The literature review gives specific information about approaches that are proving fruitful and illustrates the current level of success of the theories. Finally, an assessment is given of the status and direction of rotary-wing aerodynamic theory.

Inviscid, potential aerodynamics is the primary field for most of the advanced methods for rotors. The computational burden is still a major consideration, so many compressible and unsteady problems can be practically treated only with potential theory. Lifting surface theory solves the linearized problem, using the result for a moving singularity, often of the acceleration potential. Panel methods use surface singularity distributions to solve problems with nonlinear geometry. Transonic rotor analyses use finite difference techniques to solve the nonlinear flow equation, typically for the rotor advancing tip.

The rotor wake is a factor in almost all helicopter problems. A major question in advanced aerodynamic methods is how the wake can be included. Wake formation must at some level be considered a viscous phenomenon and the helical geometry of the helicopter wake means that the detailed structure is important even at scales on the order of the rotor size. A number of new approaches for modeling the wake are being developed. Also, the transonic blade/vortex interaction problem is being investigated as a guide for including vorticity in the flow calculations.

A useful rotor aerodynamic theory must account for the effects of viscosity, such as wake formation and blade stall, which are important for even moderate operating conditions. Navier-Stokes calculations of the entire rotor flow are well beyond present capabilities, so a hybrid method is likely to be used. Lifting line theory is still the only practical viscous method for rotors. Dynamic stall is a helicopter problem involving two-dimensional, unsteady flow with large-scale viscous effects. Dynamic stall is being analyzed using a number of advanced methods, including the solution of the turbulent, Navier-Stokes equations.

Potential Theory

Potential theory requires the assumptions that the flowfield is inviscid, irrotational, and isentropic. With concentrated vorticity in the wake and weak shocks on the rotor blades, these are normally good assumptions. In spite of the inviscid assumption, it is necessary to address in some manner wake formation, stall, and drag calculation. Often the additional assumption of incompressibility is introduced for rotor analyses, particularly for unsteady problems. Ashley and Landahl[2] and Garrick[3] provide derivations of the potential equation.

Consider a fixed reference frame (x,y,z,t), with the fluid at rest at infinity. An initially irrotational, uniform, inviscid fluid remains irrotational. Irrotationality ($\nabla \times v = 0$) implies the existence of the velocity potential ϕ, such that velocity $v = \nabla\phi$. A wing moving relative to a fluid at rest is considered because of the need to deal with rotating as well as translating wings. While v and ϕ may therefore be considered perturbations, they are not necessarily small. Introducing a coordinate system moving with the wing will influence the equations and boundary conditions, but does not change the definition of ϕ as the potential relative to the fluid at rest.

For an irrotational flow, uniform and at rest at infinity, the inviscid equation of momentum conservation integrates to Kelvin's equation:

$$\phi_t + \frac{1}{2} v^2 + \int_{p_\infty}^{p} \frac{dp}{\rho} = 0$$

Wayne Johnson received his undergraduate and graduate education at the Massachusetts Institute of Technology, obtaining a Doctor of Science degree in aeronautical engineering in 1970. He joined the U.S. Army laboratory at the Ames Research Center in 1970 and in 1981 transferred to NASA. Throughout that time, he has worked at the Ames 40×80 ft Wind Tunnel. Dr. Johnson is the author of the text *Helicopter Theory*, for which he received the Pendray Aerospace Literature Award from the AIAA. Dr. Johnson's research interests cover all disciplines associated with rotorcraft analysis and testing. For his research contributions, he has received the U.S. Department of the Army Commander's Award for Civilian Service, the NASA Medal for Exceptional Engineering Achievement, and the Grover E. Bell Award of the American Helicopter Society. His recent work has been concerned with tilt-rotor aeroelasticity, rotor wakes, and the development of a comprehensive helicopter analysis that has found wide use in the industry.

Received Feb. 22, 1985; revision received Nov. 15, 1985.

where p is the pressure and ρ the density. For isentropic flow, the local adiabatic speed of sound is $a^2=\gamma RT$, where γ is the ratio of specific heats. It follows that $p/p_\infty=(\rho/\rho_\infty)^\gamma$ and, hence, the pressure is

$$\frac{p}{p_\infty}=\left(\frac{a^2}{a_\infty^2}\right)^{\gamma/(\gamma-1)}=\left[1-\frac{\gamma-1}{a_\infty^2}\left(\phi_t+\frac{1}{2}v^2\right)\right]^{\gamma/(\gamma-1)}$$

Then, the equation for mass conservation gives

$$a^2\nabla^2\phi=-\frac{a^2}{\rho}\frac{\mathrm{D}\rho}{\mathrm{D}t}=-\frac{1}{\gamma-1}\frac{\mathrm{D}a^2}{\mathrm{D}t}$$
$$=\left(\frac{\partial}{\partial t}+v\cdot\nabla\right)\left(\phi_t+\frac{1}{2}v^2\right)$$

with $v=\nabla\phi$, and

$$a^2=a_\infty^2-(\gamma-1)\left(\phi_t+\frac{1}{2}v^2\right)$$

Thus, the equation for the velocity potential relative to still air, in tensor form, is

$$a^2\nabla^2\phi=\phi_{tt}+2\phi_{x_i}\phi_{tx_i}+\phi_{x_i}\phi_{x_j}\phi_{x_ix_j}$$

The corresponding conservative form is

$$(\rho\phi_{x_i})_{x_i}=\rho_t$$

The linearized equation of motion is the wave equation, $a_\infty^2\nabla^2\phi=\phi_{tt}$, with $(p-p_\infty)/\rho_\infty=-\phi_t$. For incompressible flow, the potential equation reduces to the Laplace equation, $\nabla^2\phi=0$, with $(p-p_\infty)/\rho_\infty=-(\phi_t+\frac{1}{2}v^2)$.

The acceleration potential ψ can be defined by considering the momentum equation: $\mathrm{D}v/\mathrm{D}t=-(\nabla p)/\rho=\nabla\psi$. Hence, $\psi=-\int(1/\rho)\mathrm{d}p=\phi_t+\frac{1}{2}v^2$, which is a nonlinear relation between the acceleration and velocity potentials. It is necessary to assume small disturbances in order to relate ψ and ϕ in a practical manner. The linearized relation is $\psi\cong-(p-p_\infty)/\rho_\infty\cong\phi_t$ and the acceleration potential is a solution of the wave equation.

The boundary condition at infinity is $v=0$ and $p=p_\infty$; hence, $\nabla\phi=\phi_t=0$, which implies $\phi=0$ (still air). For an inviscid fluid, the boundary condition at a solid body defined by the surface $F(x,t)=0$ is $\mathrm{D}F/\mathrm{D}t=F_t+v\cdot\nabla F=0$. The time derivative of $F=0$ (on the body surface) yields $F_t=-\nabla F\cdot v_b$, where v_b is the body surface velocity. Thus, the boundary condition is that there be no flow normal to the surface: $n\cdot v=\partial\phi/\partial n=n\cdot v_b$, where the body normal is $n=\nabla F/|\nabla F|$. If the body is defined by $z=g(x,y,t)$ (i.e., $F=z-g$), then the boundary condition is $v_z=g_t+v_xg_x+v_yg_y$ on $z=g$. The linearized boundary condition is $v_z\cong g_t$ on $z=0$.

A wake is a vortex surface, which allows a tangential velocity jump but no normal velocity or pressure difference: $\Delta v_n=0$ and $\Delta p=0$ (where Δ means the upper surface value minus the lower surface value). Then, Kelvin's equation gives $\Delta\phi_t+\frac{1}{2}\Delta(v^2)=0$, or $\Delta\phi_t+v_w\cdot\nabla\Delta\phi=0$ with $v_w=\frac{1}{2}(v_u+v_l)$. So the potential difference $\Delta\phi$ is constant for a point on the wake surface that is convected with the velocity v_w.

Rotating Coordinate System

Consider the transformation from inertial axes (t,r) relative to the still air, to moving axes (t',r') that contain the principle translation and rotation of the rotor (Fig. 1). Typically, the rotating y' coordinate will be the rotor blade span axis, although in fact the rotor can be placed anywhere

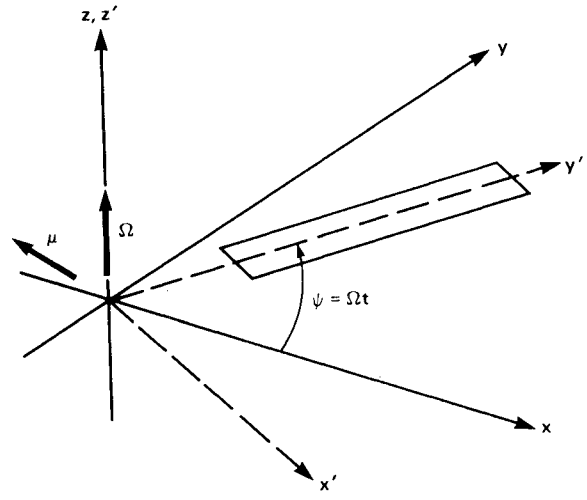

Fig. 1 Definition of rotating and translating coordinate system.

in the moving frame. The rotor is rotating at rate Ω, with the azimuth angle $\psi=\Omega t$ measured from downstream. The rotor has translation velocity V_∞ in the x-z plane, with the angle i relative to the x axis (positive for climb). So the rotation and translation vectors are

$$\Omega=(0\ 0\ \Omega)^T$$

$$\mu=\mu\Omega R(-1\ 0\ \tan i)^T$$

where $\mu=V_\infty\cos i/\Omega R$ is the advance ratio and R the rotor radius. The coordinate transformation is $r=\mu t'+\Re r'$ and $t=t'$, with the rotation matrix

$$\Re=\begin{bmatrix}\sin\psi & \cos\psi & 0\\ -\cos\psi & \sin\psi & 0\\ 0 & 0 & 1\end{bmatrix}$$

Then the derivatives are

$$\nabla=\nabla'$$

$$\frac{\partial}{\partial t}=\frac{\partial}{\partial t'}+V\cdot\nabla'$$

where V is the velocity of the air relative to the moving frame,

$$V=\frac{\partial r'}{\partial t}=-\Omega'\times r'-\mu'=\begin{bmatrix}\Omega y'+\mu\Omega R\sin\psi\\ -\Omega x'+\mu\Omega R\cos\psi\\ -\mu\Omega R\tan i\end{bmatrix}$$

Also required is the acceleration,

$$\dot V=\left(\frac{\partial}{\partial t'}+V\cdot\nabla'\right)V=\begin{bmatrix}\Omega^2x'+2\Omega V_y\\ \Omega^2y'-2\Omega V_x\\ 0\end{bmatrix}$$

After the transformation to the rotating frame has been accomplished, the primes may be omitted for simplicity.

The potential equation is transformed by substituting for the derivatives. The scalar ϕ remains a perturbation potential, although not necessarily small, defined relative to the

still air. With $U = V + \nabla\phi$, the potential equation in tensor form becomes

$$a^2 \nabla^2\phi = \left(\frac{\partial}{\partial t} + U_i \frac{\partial}{\partial x_i}\right)\left(\phi_t + V_j\phi_{x_j} + \frac{1}{2}\phi_{x_j}\phi_{x_j}\right)$$

$$= \phi_{tt} + 2U_i\phi_{tx_i} + U_iU_j\phi_{x_ix_j} + \dot{V}_i\phi_{x_i}$$

and

$$a^2 = a_\infty^2 - (\gamma - 1)(\phi_t + V_j\phi_{x_j} + \tfrac{1}{2}\phi_{x_j}\phi_{x_j})$$

As a result of rotation, the velocity V varies with time and space and Coriolis and centrifugal terms are introduced in the form of $\dot{V}$. The linearized potential equation is obtained by setting $U \cong V$. The incompressible equation is still $\nabla^2\phi = 0$.

The boundary condition on a solid body $F = 0$ becomes $F_t + U \cdot \nabla F = 0$, or $n \cdot v = \partial\phi/\partial n = n \cdot (v_b - V)$, where now v_b is the body velocity relative to the moving frame. With $F = z - g$, the boundary condition is $U_z = g_t + U_x g_x + U_y g_y$ on $z = g$, which linearizes to $v_z = g_t + V_x g_x + V_y g_y - V_z$ on $z = 0$.

Lifting Surface Theory

Lifting surface theory solves the linearized equation of motion, generally using the acceleration potential. The development provides the result for a moving singularity, which has other uses in rotary-wing theory as well.

Moving Singularity

The acceleration potential satisfies the wave equation. Moving singularities in a fixed reference frame are considered here. For a thin wing surface, $\Delta\psi = -\Delta p/\rho_\infty$, while on the wake surface $\Delta\psi = 0$. Hence, the wing is represented by a distribution of singularities over the planform. The linearized boundary condition is $\partial\phi/\partial z = w$, with the velocity potential obtained from the integral of $\phi_t = \psi$.

A solution of the wave equation is a stationary dipole at position y,

$$\psi_d = \frac{\partial}{\partial n_y}\frac{f(t - s/a)}{4\pi s}$$

where $s = x - y$, $f(t)$ is an arbitrary function of time, and $\partial(\ldots)/\partial n_y = n \cdot \nabla_y$ is the gradient in direction n. Evaluating the acceleration potential near a surface distribution of dipoles, with n the surface normal, shows that $f = \Delta\psi = -\Delta p/\rho_\infty$, the force in the normal direction. Another solution is a stationary velocity potential source,

$$\phi_s = \frac{q(t - s/a)}{4\pi s}$$

A surface distribution of sources gives $q = -\Delta(\partial\phi/\partial n)$ and hence can represent the wing thickness.

The derivation of a moving singularity follows Garrick.[3] Consider the potential at x produced by a source at $y(\tau)$, replace $f(t)$ with $f(\tau)\delta(\tau - t)$ and integrate over τ,

$$\psi_s = \int_{-\infty}^{t} \frac{f(\tau)\delta(\tau - t + s/a)}{4\pi s}\,d\tau = \frac{f}{4\pi s}\frac{d\tau}{d\tau^*}\bigg|_{\tau^*=0}$$

$$= \left[\frac{f}{4\pi s(1 - M_r)}\right]$$

where the square brackets denote the retarded time $\tau^* = 0$ or the solution of $\tau = t - s/a$ and $aM_r = -ds/d\tau = s \cdot (dy/d\tau)/s = as \cdot M/s$. Then, the moving dipole is

$$\psi_d = \left[\frac{\partial}{\partial n_y}\frac{f}{4\pi s(1 - M_r)}\right]$$

$$= \left[-\frac{f}{4\pi s^2(1 - M_r)}\frac{\partial s}{\partial n} - \frac{1}{1 - M_r}\frac{\partial}{\partial\tau}\frac{f}{4\pi as(1 - M_r)}\frac{\partial s}{\partial n}\right]$$

$$= \left[\frac{fn \cdot s}{4\pi s^3(1 - M_r)} + \frac{\partial}{\partial t}\frac{fn \cdot s}{4\pi as^2(1 - M_r)}\right]$$

Including a potential source, the result is

$$\psi = \left[\frac{fn \cdot s}{4\pi s^3(1 - M_r)} + \frac{\partial}{\partial t}\frac{fn \cdot s}{4\pi as^2(1 - M_r)} + \frac{\partial}{\partial t}\frac{q}{4\pi s(1 - M_r)}\right] \tag{1}$$

which is the acoustic formulation used by Farassat.[4] The thickness term will not be considered further here. For aerodynamic problems, the surface pressure is the unknown to be obtained from the boundary condition on the velocity potential. Integrating the acceleration potential gives the velocity potential for a moving dipole,

$$\phi_d(x, t_0) = \int_{-\infty}^{\tau_0} \frac{fn \cdot s}{4\pi s^3}\,d\tau + \frac{fn \cdot s}{4\pi as^2(1 - M_r)}\bigg|_{\tau_0} \tag{2}$$

where τ_0 is the solution of $\tau_0 = t_0 - s(\tau_0)/a$. This is the aerodynamic formulation used by Dat.[5] Farassat[6] noted the equivalence of the acoustic and aerodynamic formulations and discussed the aerodynamic applications.

Represent the wings by a surface of dipoles and apply the boundary condition to obtain a singular (Mangler-type) integral equation for the loading $f = -\Delta p/\rho_\infty$,

$$w(x, t_0) = \lim_{x \to A}\frac{\partial}{\partial n_x}\int_{\text{wings}} \phi_d\,dA(y)$$

$$= \int_{\text{wings}} \lim_{x \to A}\frac{\partial}{\partial n_x}\left\{\int_{-\infty}^{\tau_0}\frac{fn \cdot s}{4\pi s^3}\,d\tau + \frac{fn \cdot s}{4\pi as^2(1 - M_r)}\bigg|_{\tau_0}\right\}dA(y) \tag{3}$$

The integral equation for incompressible flow becomes

$$w(x, t_0) = \int_{\text{wings}} \lim_{x \to A}\left\{\int_{-\infty}^{t_0}\frac{f}{4\pi}\left(\frac{n_y \cdot n_x}{s^3} - \frac{3n_y \cdot sn_x \cdot s}{s^5}\right)d\tau\right\}dA(y) \tag{4}$$

For compressible flow, the derivative with respect to n_x can also be evaluated analytically, but the result is much more complicated. Note that the required derivatives are of the form

$$\frac{\partial}{\partial n_x}Gn_y \cdot s = Gn_y \cdot n_x + \frac{\partial G}{\partial n_x}n_y \cdot s$$

The vector s connects a point on the present wing surface (x) with a point on the wing at a retarded time y. So $n_y \cdot s = 0$ and $n_y \cdot n_x = 1$ if the wing and wake are planar. For a fixed wing, it is consistent with the linearization to neglect any warp of the wing and wake surfaces. For a rotary wing, it may also be possible to neglect the warp; the important effect of rotation is that the denominator becomes periodically small as the wake passes under the blade. With a planar wing

and wake the integral equation is

$$w(x,t_0)=\int_{\text{wings}}\left\{\int_{-\infty}^{\tau_0}\frac{f}{4\pi s^3}\,d\tau+\frac{f}{4\pi as^2(1-M_r)}\Big|_{\tau_0}\right\}dA(y)$$

A third approach, developed by Dat,[7] is to use a finite difference numerical evaluation of $\partial\phi_d/\partial n_x$. The derivative is calculated from ϕ_d evaluated at $z=\epsilon$ and 2ϵ (ϵ=2-3% chord in Ref. 8, ϵ=5% chord in Ref. 9). The potential ϕ_d has a lower-order singularity than the Mangler type of $\partial\phi_d/\partial n$. The parameter ϵ must be large enough to avoid the singularity, yet small enough for accuracy.

For steady or harmonic loading, $f=e^{i\omega t}\ell/\rho_\infty$, the magnitude of the loading factors from the integral over the wake, and the integral equation can be written in terms of a kernel function

$$w(x,t_0)=e^{i\omega t_0}\int(\ell/\rho_\infty)K\,dA(y)$$

$$K=\lim_{x\to A}\frac{\partial}{\partial n_x}\left\{\int_{-\infty}^{\tau_0}\frac{e^{i\omega(\tau-t_0)}\boldsymbol{n}\cdot\boldsymbol{s}}{4\pi s^3}\,d\tau+\frac{e^{i\omega(\tau_0-t_0)}\boldsymbol{n}\cdot\boldsymbol{s}}{4\pi as^2(1-M_r)}\Big|_{\tau_0}\right\}$$

In general, K is a function to t_0. Hence, there is interharmonic coupling for the periodic loading of a rotor blade in forward flight (each loading harmonic gives many induced velocity harmonics). When s is a function of $(t_0-\tau)$, as for fixed wings or the rotor in axial flight, the retarded time is $\tau_0=t_0-T_0$. Then, the kernel K is independent of t_0; there is no interharmonic coupling.

A lifting line theory can be obtained by applying the chordwise integral to the wing loading only. An integral equation for the section lift is obtained, with the kernel function evaluated at one chordwise location only.

Fixed Wing

The fixed-wing problem is useful as a guide and a contrast to the rotor theory, and directly for lifting line theory. Consider a thin wing on the $z=0$ plane, moving in the negative x direction and undergoing harmonic loading. Following Garrick,[3] transform now to the moving frame: $x=(x-Vt_0,y,z)^T$ and $y=(\xi-V\tau,\eta,0)^T$. The solution of $a(t-\tau)=s$ for the retarded time is $\tau=t+(M\sigma-S)/\beta^2a$, where $\sigma=x-\xi-V(t_0-t)$, $S^2=\sigma^2+\beta^2(y-\eta)^2+\beta^2z^2$, and $\beta^2=1-M^2$. The retarded distance is then $s(1-M_r)=S$. Working directly from the acceleration potential source $(\psi_s=f(\tau)/4\pi S)$ gives the integral equation, with the kernel,

$$K=\lim_{z\to 0}\frac{\partial^2}{\partial z^2}\,e^{-i\omega(x-\xi)/V}\int_{-\infty}^{x-\xi}e^{i\omega(\sigma-MS)/V\beta^2}\,\frac{d\sigma}{4\pi VS}$$

which is the form given by Watkins et al.[10]

Working from the moving dipole solution [Eq. (2)], the retarded time is required only at $t_0=t$,

$$\tau_0=t_0+[M(x-\xi)-S]/a\beta^2$$

$$S^2=(x-\xi)^2+\beta^2(y-\eta)^2+\beta^2z^2 \qquad (5)$$

So with $\sigma_0=x-\xi-V(t_0-\tau_0)=(x-\xi-MS)/\beta^2$ and $s^2=\sigma^2+(y-\eta)^2$, the kernel is

$$K=\frac{1}{4\pi V}\,e^{-i\omega(x-\xi)/V}\left(\int_{-\infty}^{\sigma_0}\frac{e^{i\omega\sigma/V}}{s^3}\,d\sigma+\frac{Me^{i\omega\sigma_0/V}}{s_0S}\right)$$

which is the form given by Landahl[11] (who credits Woodcock). The integral in K can be reduced to a function of two parameters and is a good form for series evaluation. For incompressible flow, $\sigma_0=x-\xi$. For low frequencies (exact in the steady case),

$$\int_{-\infty}^{\sigma_0}e^{i\omega\sigma/V}\,\frac{d\sigma}{s^3}+\frac{Me^{i\omega\sigma_0/V}}{s_0S}\cong\int_{-\infty}^{(x-\xi)/\beta}e^{i\omega\sigma/V}\,\frac{d\sigma}{s^3}$$

which shows that the compressible kernel is obtained by scaling $(x-\xi)$ with β in the incompressible kernel.

Rotary Wing

To complete the development of the theory for the rotary wing, the transformation to the rotating and translating coordinate system is introduced: $s=\mu(t-\tau)+\Re_t x'-\Re_\tau y'$ and $a\boldsymbol{M}=d\boldsymbol{y}/d\tau=\boldsymbol{\mu}+\boldsymbol{\Omega}\times\Re_\tau y'$, where $x'=(x,y,z)^T$, $y'=(\xi,\eta,0)^T$, and $\mu=(-\mu\Omega R,0,\lambda\Omega R)^T$. The equation for the retarded time, $a(t_0-\tau_0)=s$ (at $z=0$) becomes

$$(a^2-|\mu|^2)(t_0-\tau_0)^2+2\mu\Omega R(x\sin\Omega t_0+y\cos\Omega t_0-\xi\sin\Omega\tau_0$$
$$-\eta\cos\Omega\tau_0)(t_0-\tau_0)-[x^2+y^2+\xi^2+\eta^2-2(x\xi+y\eta)$$
$$\times\cos\Omega(t_0-\tau_0)-2(x\eta-y\xi)\sin\Omega(t_0-\tau_0)]=0$$

and then $s(1-M_r)=a(t_0-\tau_0)-s\cdot M=S$. The linearized wing is taken as the $z=0$ plane, so $\boldsymbol{n}\cdot\boldsymbol{s}=\lambda\Omega R(t-\tau)+z\cong z$ for low inflow, and on the wing $\boldsymbol{n}\cdot\boldsymbol{s}\cong 0$ (planar wing and wake assumption). The rotor consists of N separate wing surfaces. In steady forward flight, the N blades have identical, periodic loading.

The mean wake-induced velocity λ_i should be included in the vertical convection, $\lambda=\mu\tan i+\lambda_i$, when evaluating s in the kernel (but not for the boundary condition). Integrating the acceleration potential along the undisturbed air path is the equivalent to using the undistorted wake geometry defined by the translation and rotation of the coordinate system. Including λ_i in λ is a first approximation to the distorted wake geometry, needed to avoid unrealistically extreme interactions of the wing with the returning wake when the rotor angle of attack is small.

Then, for harmonic loading of the rotary wing, the kernel function is

$$K=\int_{-\infty}^{\tau_0}\frac{e^{i\omega(\tau-t_0)}}{4\pi s^3}\,d\tau+\frac{e^{i\omega(\tau_0-t_0)}}{4\pi as^2(1-M_r)}\Big|_{\tau_0}$$

The distance s is a function of t_0, τ, x', and y'. Even in the steady case, there is no simple analytical evaluation of the integral over the helical wake. It is necessary to evaluate a transcendental equation for the retarded time τ_0. In forward flight the kernel is a function of t_0, but in axial flight the retarded time can be written $\tau_0=t_0-T_0(x',y')$. In terms of polar coordinates ($x=r\sin\Theta$, $y=r\cos\Theta$, $\xi=\rho\sin\theta$, $\eta=\rho\cos\theta$), the kernel for axial flow is

$$K=\frac{1}{4\pi\Omega}\,e^{-i\omega(\Theta-\theta)/\Omega}\left(\int_{-\infty}^{\sigma_0}\frac{e^{i\omega\sigma/\Omega}}{s^3}\,d\sigma+\frac{\Omega e^{i\omega\sigma_0/\Omega}}{as_0S}\right)$$

where $\sigma_0=\Theta-\theta-\Omega(t_0-\tau_0)$ and

$$s^2=(\lambda R)^2(\sigma-\Theta+\theta)^2+r^2+\rho^2-2r\rho\cos\sigma$$

$$(a\beta_\lambda/\Omega)^2(\sigma_0-\Theta+\theta)^2-(r^2+\rho^2-2r\rho\cos\sigma_0)=0$$

$$S=(a\beta_\lambda^2/\Omega)(\sigma_0-\Theta+\theta)+(\Omega/a)r\rho\sin\sigma_0$$

$$\beta_\lambda^2=1-(\lambda\Omega R/a)^2$$

This result is superficially similar to the fixed-wing kernel, but the differences are significant. The use of rectangular coordinates is more appropriate for typical helicopter blade

planforms. The integral in the kernel is a function of five parameters, not two; and a series evaluation will not work as well as for the fixed wing, because s is periodically small. Even in the steady, axial flow case, a transcendental equation must be solved for the retarded time. Even for incompressible flow, when the retarded time is not needed, the kernel involves an integral over the helical wake geometry. In forward flight, the kernel introduces interharmonic coupling. While the lifting surface problem as formulated is much simpler for axial flight, in hover the wake geometry is so important that the wake contraction, wake convection, and blade/vortex interaction have a first-order influence on the loading.

Under the assumption that the retarded time is small, an analytical solution can be obtained

$$\tau_0 \cong t_0 + (\boldsymbol{V}\cdot(\boldsymbol{x}'-\boldsymbol{y}')/a - S)/a\beta^2$$

where

$$S^2 = (\boldsymbol{V}\cdot(\boldsymbol{x}'-\boldsymbol{y}')/a)^2 + \beta^2|\boldsymbol{x}'-\boldsymbol{y}'|^2$$

$$\beta^2 = 1 - (|\boldsymbol{V}|^2 + \dot{\boldsymbol{V}}\cdot(\boldsymbol{x}'-\boldsymbol{y}'))/a^2$$

and $s(1-M_r)=S$. Here, $\boldsymbol{V}$ and $\dot{\boldsymbol{V}}$ are the velocity and acceleration of the coordinate system at the observer point $\boldsymbol{x}$ (and are functions of t_0). Except for the acceleration term in β^2, this is the solution for a fixed wing at velocity $\boldsymbol{V}(\boldsymbol{x})$. It illustrates the dependence of $(\tau_0 - t_0)$ on t_0 for forward flight, but not for axial flight. For axial flow and polar coordinates, the result is

$$\tau_0 = t_0 + [(\Omega/a)r\rho\sin(\Theta-\theta) - S]/a\beta^2$$

$$S^2 = (\Omega/a)^2[r\rho\sin(\Theta-\theta)]^2 + \beta^2[r^2+\rho^2-2r\rho\cos(\Theta-\theta)]$$

$$\beta^2 = 1 - (\Omega/a)^2[\lambda^2R^2 + r\rho\cos(\Theta-\theta)] \qquad (6)$$

which with the additional assumption of small $(\Theta-\theta)$ was given by Sopher.[12] An alternate form for the general case is

$$\tau_0 = t_0 + \{\tfrac{1}{2}[\boldsymbol{V}(\boldsymbol{x})+\boldsymbol{V}(\boldsymbol{y})]\cdot(\boldsymbol{x}'-\boldsymbol{y}')/a - S\}/a\beta^2$$

$$S^2 = \{\tfrac{1}{2}[\boldsymbol{V}(\boldsymbol{x})+\boldsymbol{V}(\boldsymbol{y})]\cdot(\boldsymbol{x}'-\boldsymbol{y}')/a\}^2 + \beta^2|\boldsymbol{x}'-\boldsymbol{y}'|^2$$

$$\beta^2 = 1 - \boldsymbol{V}(\boldsymbol{x})\cdot\boldsymbol{V}(\boldsymbol{y})/a^2$$

where $\boldsymbol{V}(\boldsymbol{x})$ and $\boldsymbol{V}(\boldsymbol{y})$ are the velocities of the observer and source points, respectively. Since $\boldsymbol{V}(\boldsymbol{y})$ depends on τ, this is not really a solution for the retarded time, except in axial flight where the velocities do not depend on time. The above approximations are based on $\Omega(t-\tau)\ll 1$, which with $a(t-\tau)=s$ implies $s\Omega/a\ll 1$, or $M_{tip}(s/R)\ll 1$. This requirement might be valid even at high tip Mach numbers, since the kernel is dominated by small s/R. It is an interesting possibility that this approximate solution might be good up to the point where nonlinear transonic equations are needed. However, in practice, a numerical solution of the exact equation for the retarded time may require little additional computation effort.

Table 1 summarizes the work that has been done on lifting surface theory for helicopter rotors.[5,7-9,12-17] Dat[5,7,8] and Costes[9,13] used a series representation of the loading, a finite difference evaluation of $\partial\phi/\partial n$, and included λ_i when calculating s. Runyan and Tai[16,17] used a doublet lattice representation of the loading and an analytical evaluation of $\partial\phi/\partial n$. Hanson[14,15] transformed the kernel from an integral over the wake with a transcendental equation for the retarded time to an infinite sum of integrals over the Bessel functions by introducing a Fourier transform over the wake age in helical coordinates.

Panel Methods

Panel methods use a surface singularity distribution to solve the linear potential equation for arbitrary geometry. The use of the velocity potential for inviscid, irrotational flow reduces the problem to the solution of an integral equation for a scalar function on a two-dimensional surface. The derivation is usually based on Green's theorem. Most of the work for helicopters has dealt with incompressible flow, for which the equation of motion is linear without further approximation and the unsteadiness enters only through the boundary conditions and the wake.

Surface Singularity Representations

The derivation of the incompressible integral equation will follow Lamb.[18] The velocity potential satisfies Laplace's equation, $\nabla^2\phi=0$, in either the fixed or moving frame. The boundary condition is that $\partial\phi/\partial n = w$ on the body surface and the potential jump in the wake is convected from the trailing edge. Assume ϕ and ψ are single-valued functions satisfying Laplace's equation in a volume V bounded by a surface A. Using Green's theorem and substituting for Laplace's equation gives

$$\oint\left(\phi\frac{\partial\psi}{\partial n} - \psi\frac{\partial\phi}{\partial n}\right)dA = -\int(\phi\nabla^2\psi - \psi\nabla^2\phi)dV = 0$$

For multiply connected regions (e.g., in two-dimensional problems or for an actuator disk), branch cuts and corresponding circulations can be introduced. Let ψ be a unit source $\boldsymbol{x}$: $\psi = 1/(4\pi s)$, where $s=\boldsymbol{x}-\boldsymbol{y}$. The volume V is the space external to the body and wake, excluding a small sphere around the singularity at $\boldsymbol{x}$. Evaluating the surface integral over this small sphere gives

$$4\pi\phi(\boldsymbol{x}) = \int\left(\phi\frac{\partial}{\partial n}\frac{1}{s} - \frac{1}{s}\frac{\partial\phi}{\partial n}\right)dA(\boldsymbol{y}) \qquad (7)$$

which is a representation of ϕ as a surface distribution of sources and doublets. This is an integral equation, since it is not possible to specify both ϕ and $\partial\phi/\partial n$ on the surface. If the point $\boldsymbol{x}$ is inside the body (outside V), the left-hand side

Table 1 Rotary-wing lifting surface theory

Ref.	Eq.	Wing model	Compressibility	Comments
12	(1)	Thickness	Comp.	Axial/steady; polar coordinates
7	(4), Ref. 8	Lifting line	Incomp./comp.	Polar coordinates
8	—	Lifting surface	Incomp./comp.	
5	(2)	Lifting surface	Comp.	Helical coordinates
9	Ref. 8	Lifting line	Comp.	
13	(2)	Lifting line	Comp.	
14,15	—	Lifting surface	Comp.	Axial/steady; helical coordinates
16	(4)	Lifting line	Incomp.	
17	(3)	Lifting surface	Incomp./comp.	

of Eq. (7) is zero. The integral of the dipole distribution is singular as x approaches the surface. Accounting for the singular part (excluding a small circle about x), the left-hand side becomes $2\pi\phi$.

To obtain a representation in terms of sources or doublets alone, consider the potential ϕ' of an arbitrary flow inside the body. For x outside the body, then

$$0=\int\left(\phi'\frac{\partial}{\partial n}\frac{1}{s}-\frac{1}{s}\frac{\partial\phi'}{\partial n}\right)dA(y)$$

so

$$4\pi\phi(x)=\int\left[(\phi-\phi')\frac{\partial}{\partial n}\frac{1}{s}-\frac{1}{s}\left(\frac{\partial\phi}{\partial n}-\frac{\partial\phi'}{\partial n}\right)\right]dA(y) \quad (8)$$

For a source representation, let $\phi=\phi'$ on the surface,

$$4\pi\phi(x)=-\int\frac{1}{s}\left(\frac{\partial\phi}{\partial n}-\frac{\partial\phi'}{\partial n}\right)dA(y)=-\int\frac{\sigma}{s}\,dA(y) \quad (9)$$

so the tangential velocity is continuous and the normal velocity discontinuous at the surface. For a doublet representation, let $\partial\phi/\partial n=\partial\phi'/\partial n$ on the surface,

$$4\pi\phi(x)=\int(\phi-\phi')\frac{\partial}{\partial n}\frac{1}{s}\,dA(y)=\int\sigma\frac{\partial}{\partial n}\frac{1}{s}\,dA(y) \quad (10)$$

so the tangential velocity is discontinuous and the normal velocity continuous at the surface.

The surface must be collapsed into a thin layer in order to model a wake and for the thin-wing approximation. For a thin layer, the surface integral will be taken over the upper surface only and the integrand will be the difference between the upper and lower surface singularity strengths. With a source distribution, $\Delta\sigma=\Delta\partial\phi/\partial n$ and $\Delta\phi=0$. The tangential velocity is the same on both sides, so sources can represent the wing thickness, but cannot be used to model a wake. With a double distribution, $\Delta\sigma=\Delta\phi$ and $\Delta\partial\phi/\partial n=0$. The normal velocity is the same on both sides, but the tangential velocity can jump. A doublet distribution is a vortex sheet, which can represent a wake or a lifting wing without thickness. For a thin layer, Eq. (7) involves only $\Delta\partial\phi/\partial n=\Delta w$, so the lifting boundary condition is lost. An integral equation based on Eq. (7) is not proper for a thin wing.

Integral Equation

Evaluating x in Eq. (7) on the surface produces an integral equation for ϕ on the surface,

$$2\pi\phi(x_s)=\int_{\text{body}}\left[\phi(y_s)\frac{\partial}{\partial n}\frac{1}{s}-\frac{1}{s}\frac{\partial\phi}{\partial n}\right]dA(y)+\int_{\text{wake}}\Delta\phi\frac{\partial}{\partial n}\frac{1}{s}\,dA(y) \quad (11)$$

The wing boundary condition gives $\partial\phi/\partial n$ and $\Delta\phi$ in the wake is convected from the trailing edge. Most recent methods are based on this equation.[19] Generally, both the integral equation and the dependent variable (potential rather than velocity) are well behaved, producing a well-conditioned numerical problem,[20] even for cases such as a wake cutting another body.[21] Other integral equations (discussed below) involve higher-order singularities for lifting problems. Equation (11) is not applicable to thin wings, but practical thicknesses present no difficulties.[22] Note that the singular part of the doublet integral has already been included on the left-hand side. For a flat, constant-strength panel, there is no more contribution than the singular part produced by the local panel; hence, the singularity of the integral is of no concern.

A panel method is produced when the surface is approximated by a connected set of small elements. Typically, the panels are quadrilaterals; sometimes the panels are approximated by flat quadrilaterals or triangles. Usually, the singularity strength is constant over a panel. Note that a constant-strength doublet panel representation is equivalent to a vortex lattice. Higher-order distributions are also used,[19] but constant-strength panels are much more efficient and are generally satisfactory for subsonic flow. The integral equation is evaluated at collocation points, normally the panel centers. Thus, a set of algebraic equations for the potential ϕ_k on the panels is obtained,

$$2\pi\phi_k=\sum_{\text{body}}A_{kj}\phi_j+\sum_{\text{body}}B_{kj}\left(\frac{\partial\phi}{\partial n}\right)_j+\sum_{\text{wake}}D_{kj}\Delta\phi_j$$

The influence coefficients depend only on the geometry (not the boundary conditions) and, hence, are fixed for rigid-body motion and a prescribed wake geometry.

To evaluate the pressure, ϕ_t and the velocity $\nabla\phi$ are required (probably in the moving frame). On the body, the boundary condition defines the normal velocity and the tangential velocity; ϕ_t can be obtained by numerical differentiation of the surface potential. A piecewise constant representation of ϕ must be fit to a polynomial distribution over several nearby panels before being differentiated.

In practice, the Kutta condition or Joukowski hypothesis is implemented by attaching the wake to the wing trailing edge (thereby specifying where the vorticity leaves the body), evaluating the wake strength from $\Delta\phi$ of the panels at the trailing edge, and convecting $\Delta\phi$ in the wake with the local velocity (for an undistorted wake geometry, approximated by the freestream). The theory behind the Kutta condition, although incomplete, is more complex and subtle than practice would suggest. Mangler and Smith[23] showed that at a finite angle trailing edge, the wake should be tangent to the upper or lower surface, depending on local flow conditions. The implications for a panel method have been discussed by Refs. 24-26. It appears that the trailing-edge bisector can usually be used for the wake direction. It is important that the Kutta condition be used in a form such that the results are not sensitive to the geometric details of its implementation.

Other integral equations can be obtained from Eqs. (8-10) by evaluating the normal derivative of the potential $\partial\phi/\partial n_x$ on the body surface,

$$4\pi\frac{\partial\phi}{\partial n_x}=-\int\sigma\frac{\partial}{\partial n_x}\frac{1}{s}\,dA(y)=2\pi\sigma(x)-\int\sigma\frac{\partial}{\partial n_x}\frac{1}{s}\,dA(y) \quad (12)$$

$$4\pi\frac{\partial\phi}{\partial n_x}=\int\sigma\frac{\partial^2}{\partial n_x\partial n_y}\frac{1}{s}\,dA(y) \quad (13)$$

$$4\pi\frac{\partial\phi}{\partial n_x}=\int\left(\sigma_d\frac{\partial^2}{\partial n_x\partial n_y}\frac{1}{s}-\sigma_s\frac{\partial}{\partial n_x}\frac{1}{s}\right)dA(y) \quad (14)$$

In each case, $\partial\phi/\partial n_x$ is evaluated from the boundary condition and the equation is solved for the singularity strength σ. A source distribution cannot represent a wake, so Eq. (12) is applicable only to nonlifting bodies. The second form of Eq. (12) shows the singular part of the integral. For a flat,

constant-strength panel, there is no more contribution from the local panel, so the singularity is of no concern. The doublet distribution [Eq. (13)] can represent a lifting wing (but not thickness if the wing surface is modeled as a thin layer). On a wake, the singularity difference is convected from the trailing edge. Equation (13) has a Mangler-type singularity, which is of higher order than the singularities in Eqs. (11) and (12) and which requires more care to evaluate. However, a constant-strength doublet panel is equivalent to a vortex lattice, for which the singularity is of no concern. The combination of source and doublet singularities [Eq. (14)] is not a unique representation. It is necessary to prescribe the distribution of the doublet or source strength over the body or to add boundary conditions to the problem. Such flexibility can be used to improve the numerical conditioning of the integral equation. To obtain the velocity and pressure, even on the body surface, it is necessary to integrate the singularity distribution over the entire body (unless the thin-wing model is used).

Compressible Flow

Helicopter rotor blades normally operate at speeds involving compressible flow. For a helicopter fuselage, separation rather than compressibility effects are the primary concern. Consider subsonic potential flow with an arbitrary geometry. The small perturbation velocity potential (relative still air) satisfies the wave equation: $a^2\nabla^2\phi=\phi_{tt}$. The derivation of the integral equation will be guided by Morse and Feshback,[27] where Green's function was used to solve the problem for a fixed body.

Using Green's theorem, substituting for the wave equation, and then bringing the time derivative outside the volume integral for a moving body, gives

$$\int\left(\phi\frac{\partial\psi}{\partial n}-\psi\frac{\partial\phi}{\partial n}\right)\mathrm{d}A=-\int(\phi\nabla^2\psi-\psi\nabla^2\phi)\mathrm{d}V$$

$$=-\frac{1}{a^2}\int(\phi\psi_{\tau\tau}-\psi\phi_{\tau\tau})\mathrm{d}V$$

$$=-\frac{1}{a^2}\int(\phi\psi_\tau-\psi\phi_\tau)_\tau\mathrm{d}V$$

$$=-\frac{1}{a^2}\frac{\partial}{\partial\tau}\int(\phi\psi_\tau-\psi\phi_\tau)\mathrm{d}V$$

$$+\frac{1}{a^2}\int\frac{\partial F}{\partial\tau}\frac{1}{|\nabla F|}\times(\phi\psi_\tau-\psi\phi_\tau)\mathrm{d}A$$

The body is defined by $F=0$, and so

$$\frac{\partial F}{\partial\tau}\frac{1}{|\nabla F|}=-\boldsymbol{n}\cdot\frac{\partial\boldsymbol{y}}{\partial\tau}=-a\boldsymbol{n}\cdot\boldsymbol{M}$$

where $\boldsymbol{n}$ is the body normal and $\boldsymbol{M}$ the surface Mach number. Let $\psi=\delta(\tau^*)/4\pi s$, where $\tau^*=\tau-t+s/a$, and $s=x-y$. Then ψ is singular at x, so the volume V must exclude a small sphere around x. Evaluating the singular part of the left-hand side integral over the surface around x gives $-\phi(x,\tau)\delta(\tau-t)$. Next, the equation is integrated over time, from $\tau=-\infty$ to ∞. The remaining volume integral is zero, since $\phi=\phi_\tau=0$ at $\tau=-\infty$, and $\psi=\psi_\tau=0$ at $\tau=\infty$. To proceed further, the order of the time and area integrations is interchanged. First, it is necessary to transform to a moving coordinate frame, $y'=h(y,\tau)$ and $\tau'=\tau$, such that the body surface $F=0$ is not a function of τ'. The time derivative transforms as

$$\frac{\partial}{\partial\tau}=\frac{\partial}{\partial\tau'}+\boldsymbol{V}\cdot\nabla'\equiv\frac{\mathrm{d}}{\mathrm{d}\tau'}$$

where $\boldsymbol{V}=\partial\boldsymbol{h}/\partial\tau$ is the velocity of the air relative to the moving frame. For rigid-body motion, a rotating and translating (and in general acclerating) coordinate transformation is required, such as derived above for the rotor. For a flexible body the transformation would be more complex. Hence,

$$\phi(x,t)=\int\int_{-\infty}^{\infty}\left[\left(\phi\frac{\partial\psi}{\partial n}-\psi\frac{\partial\phi}{\partial n}\right)-\frac{\mathrm{d}F}{\mathrm{d}a\tau'}\frac{1}{|\nabla F|}\left(\phi\frac{\mathrm{d}\psi}{\mathrm{d}a\tau'}-\psi\frac{\mathrm{d}\phi}{\mathrm{d}a\tau'}\right)\right]\mathrm{d}\tau'\mathrm{d}A(y')$$

To transform ψ to the moving frame, note that $\tau^*=\tau'-t+s(\tau')/a$. So $\delta(\tau^*)=\delta(\tau'-\tau_r)\partial\tau'/\partial\tau^*=\delta(\tau'-\tau_r)\div(1-M_r)$, where the retarded time τ_r is the solution to $\tau^*=0$. Finally, $\psi=\delta(\tau'-\tau_r)/4\pi s(1-M_r)$.

Thus, the integral equation for a moving body in compressible flow is

$$4\pi\phi(x,t)=\int\left[\left(\phi\frac{\partial}{\partial n}\frac{1}{s(1-M_r)}+\frac{\partial\tau_r}{\partial n}\frac{\partial}{\partial\tau'}\frac{\phi}{s(1-M_r)}-\frac{1}{s(1-M_r)}\frac{\partial\phi}{\partial n}\right)-\frac{\mathrm{d}F}{\mathrm{d}a\tau'}\frac{1}{|\nabla F|}\left(\phi\frac{\mathrm{d}}{\mathrm{d}a\tau'}\frac{1}{s(1-M_r)}-\frac{\partial}{\partial\tau'}\frac{\phi}{s(1-M_r)}\frac{\mathrm{d}(\tau'-\tau_r)}{\mathrm{d}a\tau'}-\frac{1}{s(1-M_r)}\frac{\mathrm{d}\phi}{\mathrm{d}a\tau'}\right)\right]\mathrm{d}A(y')$$

$$4\pi\phi(x,t)=\int\left[\left(\phi\frac{\partial}{\partial n}\frac{1}{S}-\frac{1}{1-M_r}\frac{\partial s}{\partial n}\frac{\partial}{\partial a\tau'}\frac{\phi}{S}-\frac{1}{S}\frac{\partial\phi}{\partial n}\right)-\boldsymbol{n}\cdot\boldsymbol{M}\left(\phi\,\boldsymbol{M}\cdot\nabla\frac{1}{S}+\frac{\partial}{\partial a\tau'}\frac{\phi}{S}\frac{M_r}{1-M_r}-\frac{1}{S}\boldsymbol{M}\cdot\nabla\phi+\frac{2}{S}\frac{\partial\phi}{\partial a\tau'}\right)\right]\mathrm{d}A(y')$$

where the square brackets imply evaluation at the retarded time and $S=s(1-M_r)$. For x on the body surface, the left-hand side becomes $2\pi\phi$ when the singular part of the right-hand side is accounted for. The surace $A(y')$ includes both wings and wakes. Collapsing the wake to a thin layer gives integrals of the potential jump $\Delta\phi$ over the wake surface. The first two terms on the right-hand side are recognized as the moving dipole and the third term is a moving source. The operator $(\boldsymbol{n}\cdot\nabla-\boldsymbol{n}\cdot\boldsymbol{M}\boldsymbol{M}\cdot\nabla)$ accounts for the normal on the moving body. For zero body slope in the flow direction, $\boldsymbol{n}\cdot\boldsymbol{M}=0$, only the first three terms remain on the right-hand side and the result is just an extension of the incompressible equation using moving singularities. For a thin wing, $\boldsymbol{n}\cdot\boldsymbol{M}\cong 0$ can be a good approximation. For a fixed body, the equation becomes

$$4\pi\phi(x,t)=\int\left[\phi\frac{\partial}{\partial n}\frac{1}{s}-\frac{\partial\phi}{\partial\tau}\frac{1}{as}\frac{\partial s}{\partial n}-\frac{\partial\phi}{\partial n}\frac{1}{s}\right]_{\tau=t-s/a}\mathrm{d}A(y)$$

which is Kirchhoff's equation, a mathematical statement of Huygen's principle.[3,18,27] Morino[22] argues that small motion of the wing relative to a basic moving frame can be neglected in the integral equation (but, of course, not in the boundary condition).

For a fixed wing, $M=-iM$ (neglecting motion relative to the uniform flight speed); so $s(1-M_r)=S$ and $\tau_r=t-T$, where S and T are constants defined by Eq. (5). The integral equation becomes

$$4\pi\phi(x,t)=\int\Big[\Big(\phi\frac{\partial}{\partial n}\frac{1}{S}-\frac{\dot\phi}{S}\frac{\partial T}{\partial n}-\frac{1}{S}\frac{\partial\phi}{\partial n}\Big)-\frac{dF}{da\tau'}\frac{1}{|\nabla F|}\Big(\phi M\frac{\partial}{\partial\xi}\frac{1}{S}-\frac{\dot\phi}{S}M\frac{\partial T}{\partial\xi}-\frac{1}{S}M\frac{\partial\phi}{\partial\xi}-\frac{2\dot\phi}{aS}\Big)\Big]_{\tau=t-T}dA(y') \tag{15}$$

$$4\pi\phi(x,t)=\int\Big[\Big(\phi\frac{\partial}{\partial n}\frac{1}{S}-\frac{\dot\phi}{aS(1-M_r)}\frac{\partial s}{\partial n}-\frac{1}{S}\frac{\partial\phi}{\partial n}\Big)-n\cdot iM\Big(\phi M\frac{\partial}{\partial\xi}\frac{1}{S}-\frac{\dot\phi M_r}{aS(1-M_r)}-\frac{1}{S}M\frac{\partial\phi}{\partial\xi}-\frac{2\dot\phi}{aS}\Big)\Big]_{\tau=t-T}dA(y')$$

Morino[22] derived Eq. (15). For steady flow, the result becomes

$$4\pi\phi(x)=\int\Big[\phi\Big(\frac{\partial}{\partial n}-M^2\boldsymbol{i}\cdot\boldsymbol{n}\frac{\partial}{\partial\xi}\Big)\frac{1}{S}-\frac{1}{S}\Big(\frac{\partial\phi}{\partial n}-M^2\boldsymbol{i}\cdot\boldsymbol{n}\frac{\partial\phi}{\partial\xi}\Big)\Big]dA(y')$$

The substitution $x=\beta\bar{x}$, $\xi=\beta\bar{\xi}$ scales this to the solution of the incompressible problem $\bar\nabla^2\phi=0$, with $S=\bar{s}/\beta$ and

$$\frac{\partial}{\partial n}-M^2\boldsymbol{i}\cdot\boldsymbol{n}\frac{\partial}{\partial\xi}=\frac{\partial}{\partial\bar n}$$

identified as the body normal derivative in the scaled coordinate frame. The Prandtl-Glauert scaling is obtained if the body slope is zero (or negligibly small) in the flow direction, so $\boldsymbol{n}=\bar{\boldsymbol{n}}$.

Literature

The foundations of panel methods are in fixed-wing applications. Hess and Smith[28] pioneered the use of Eq. (12) for steady, nonlifting bodies. Rubbert and Saaris[29,30] and Hess[24] developed Eq. (14) for steady lifting problems, using a surface distribution of sources and an internal or surface distribution of doublets. Djojodihardjo and Widnall[31] used Eq. (13) for unsteady problems. Morino[22] and Morino and Kuo[32] developed a panel method for unsteady, compressible flow based on Eq. (15). Maskew[20,33] developed a panel method based on Eq. (11). The purpose here is not to review all panel methods, but rather those that have been applied or developed for helicopter problems.

Table 2 summarizes the work that has been done with panel methods for helicopter rotors.[21,25,26,33-59] Helicopter fuselages are analyzed to determine the body flow and the velocity induced at a rotor. Appropriately for helicopters, the methods used have been incompressible, but there have been many attempts to include a model of separated flow. Some of the methods[33,34] used just a boundary-layer calculation. The separation models that have been developed include: mass injection on the body surface within the separated region[37]; a vortex shear layer, with an isolated vortex line to enforce stagnation at the prescribed separation line[41]; a boundary-layer calculation of the separation line

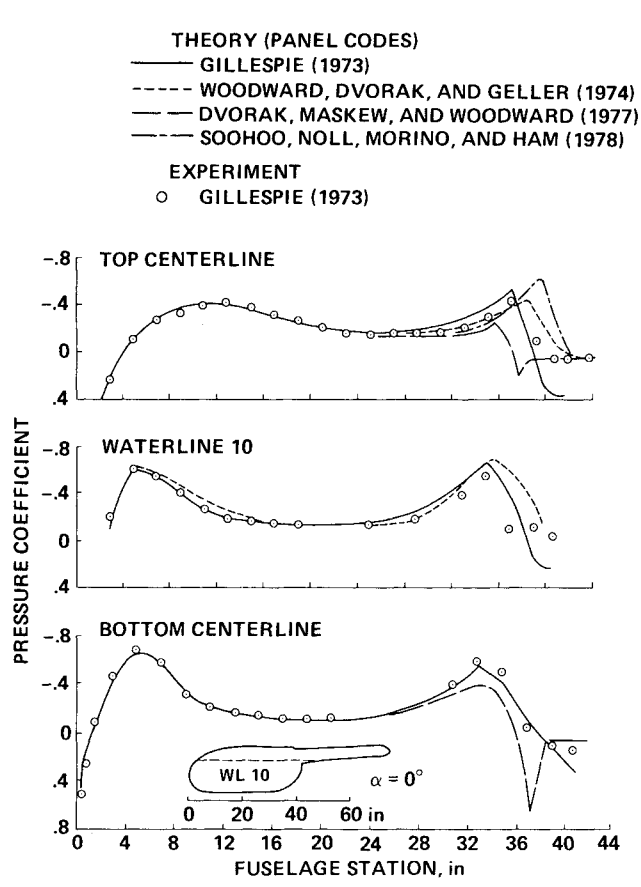

Fig. 2 Helicopter fuselage air loading calculated using panel methods.[34,37,38,41]

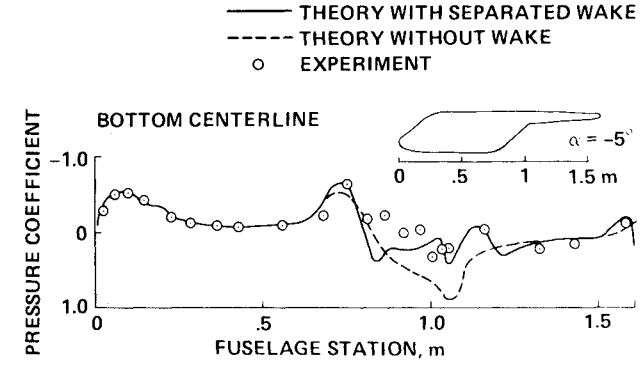

Fig. 3 Helicopter fuselage air loading calculated using panel methods.[42]

and a volume distribution of vorticity within the separated wake[42]; and a boundary-layer calculation of the separation line, with a vortex shear layer for the separated wake boundary.[38,39] The latter model has also been used by Maskew and Dvorak[45] and Costes[46] to calculate the maximum lift of a two-dimensional airfoil with trailing-edge separation. Figures 2 and 3 compare the results from several of these methods with the pressures measured on model helicopter fuselages.

The application of panel methods to coupled rotor/body aerodynamics have used an actuator disk model of the rotor, so that the problem remains steady. Freeman[47] calculated the wake-induced velocity from a prescribed rotor loading and wake geometry and included these velocities in the body surface boundary condition. The influence of the body on the rotor was not calculated. Clark and Maskew[21,48] modeled the rotor as a thin circular wing with prescribed strengths of sources (for the induced velocity) and doublets (for the

loading) and with the wake trailed from the circumference. The calculation iterated between the rotor and the body, including the body-induced velocity in the rotor loading analysis. The code was well behaved if the rotor wake cut the body [an advantage of using Eq. (11)], but the model was considered physically realistic only with the body entirely inside or entirely outside the rotor wake. Comparisons with measured velocities and pressures for a simple rotor/body configuration[60] suggested that an unsteady analysis is required even to calculate the mean flowfield.

All of the applications of panel methods to rotary wings have been for hover, which is a steady problem. The rotor flow is really compressible, but the analyses have been incompressible, with several methods to approximate the effects of Mach number: modification of the wing self-induced velocity to correct the lift-curve slope for compressibility and real flow effects[51]; an approximate transformation to the incompressible equation, similar to the Prandtl-Glauert transformation[52]; and use of the approximate compressible singularity [Eq. (6)].[53,55] The wake geometry is particularly important for hover; a number of the panel methods have included free-wake geometry calculations (see Table 2). A far-wake model is needed for efficiency[52,53,55] Figure 4 presents hovering rotor blade section loading calculated using panel methods. The experimental data show the effects of the different tip vortex roll-up for the two tip shapes. Summa[54] attempted to model (not calculate) the roll-up; Shenoy and Gray[56] did not. Figure 5 compares hovering rotor blade loading as calculated by lifting line theory, lifting surface theory, and a panel method. Comparisons with experiment (for example, Ref. 61) have not demonstrated a completely satisfactory theory. Wake geometry calculations and measurements are needed to improve hovering rotor theories.

Transonic Theory

Transonic rotor analyses use finite difference techniques to solve the nonlinear equations for the flow about the advancing blade tip. Although a hovering rotor can be analyzed, transonic flow is normally encountered on rotors in high-speed forward flight. It follows that the problem is unsteady:

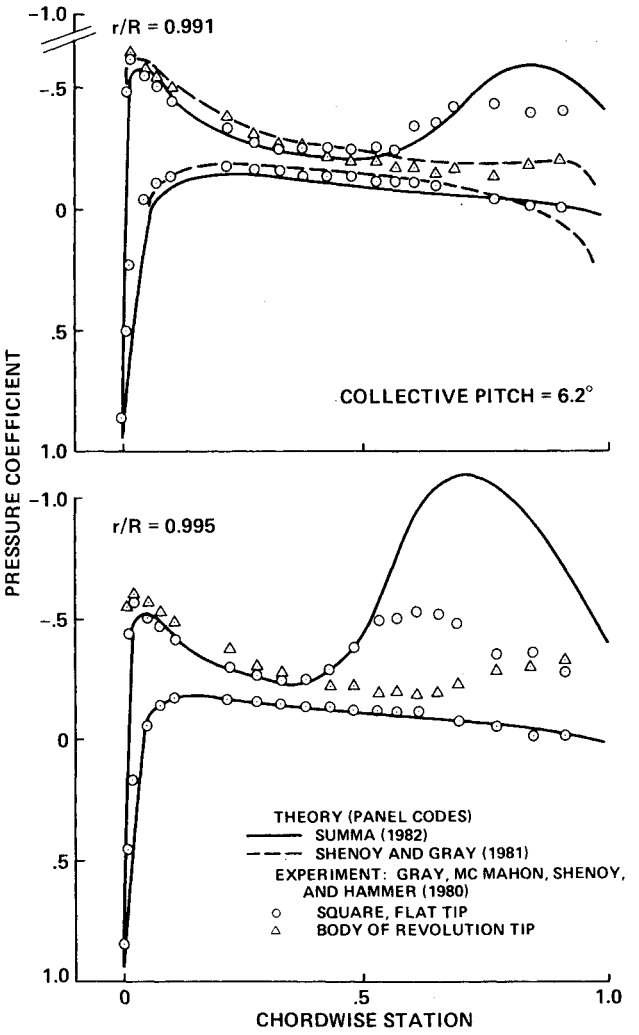

Fig. 4 Hovering rotor tip loading calculated using panel methods.[54,56]

Table 2 Rotary-wing panel methods

Ref.	Eq.	Steady or unsteady	Free wake	Comments
			Fuselage	
34-36	12	S	No	—
37-39	14	S	No	WBAERO; separated flow model
40	14	S	No	—
41	11	U	No	Separated flow model
42	12	S	No	Separated flow model
33	11	S	Yes	VSAERO
			Components	
43	11	U	Yes	Tip vortex formation
44	11	U	Yes	Oscillating wing tip
45	13	S	Yes	Two-dimensional stall
46	11	U	No	Two-dimensional stall
			Rotor/Body	
47	12	S	No	—
21,48,49	11	S	Yes	ROTBOD (VSAERO for body)
			Hovering rotor	
50	13	S	No	—
26	13	U	Yes	—
51,52	13	S	No	Thin wing; compressibility approximation
53,54	13	S	Yes	Hover; thin wing; compressibility approx.
54,55	11	S	No	ROTAIR (HOVER wake geom.); comp. approx.
56	13	S	Yes	—
57,58	11	U	No	—
25,59	11	U	Yes	—

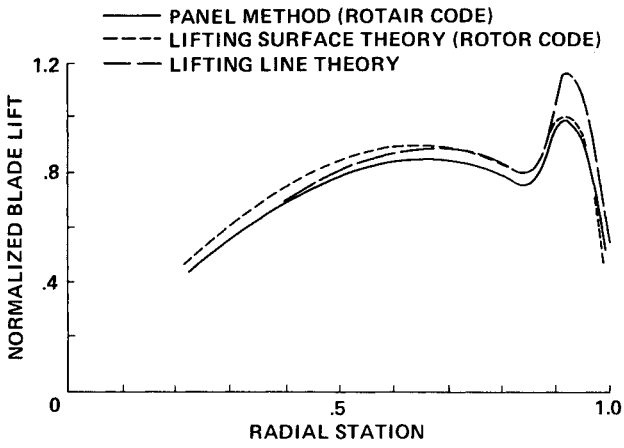

Fig. 5 Hovering rotor blade loading calculations.[53,55]

there is a once-per-revolution variation in the velocity seen by the blade (corresponding to a low reduced frequency), as well as higher harmonics from the blade surface boundary conditions. In the investigations reported to date, primarily the potential equation has been considered. In spite of the fact that shocks are not isentropic, the potential equation is a good approximation up to a local normal-shock Mach number of about 1.3; when the error resulting from the isentropic assumption is large, the inviscid assumption is probably also bad.[62]

The equation for the velocity potential relative to the still air as derived for a rotating and transisting coordinate system is

$$a^2\nabla^2\phi=\phi_{tt}+2U_i\phi_{tx_i}+U_iU_j\phi_{x_ix_j}+\dot{V}_i\phi_{x_i}$$

$$a^2=a_\infty^2-(\gamma-1)(\phi_t+V_j\phi_{x_j}+\tfrac{1}{2}\phi_{x_j}\phi_{x_j})$$

$$p/p_\infty=(a^2/a_\infty^2)^{\gamma/(\gamma-1)} \tag{16}$$

with the boundary condition $U_z=g_t+U_xg_x+U_yg_y$ on $z=g$. In full potential methods, this exact equation and tangent boundary condition are solved. The complexity of the differential equation and the need for a body-fitted grid transformation imply a significant computational effort.

Small-Disturbance Equation

The equation for small disturbances is useful both to understand the essential character of the problem and to reduce the computational effort. The small-disturbance equation is itself simpler than the full potential equation and the linearized boundary condition means that a simpler grid can be used. The small-disturbance approximation is generally valid for moderate airfoil thickness and angle of attack, but is always incorrect at the leading edge. The derivation of the small-disturbance equation will be guided by Isom.[63]

The small parameter τ will be a measure of the disturbance produced by the wing thickness and angle of attack. Hence, the wing surface is defined by $g\triangleq c\tau$, where c is the blade chord. Let the order of the velocity potential be defined by the small parameter δ, such that $\phi\triangleq\Omega Rc\delta$. The chord and tip speed are measures of the displacement and velocity in the chordwise disrection: $x\triangleq c$ and $V_x\triangleq\Omega R$. Small disturbance implies a linearized boundary condition: $V_z+\phi_z=g_t+V_xg_x+V_yg_y$ on $z=0$. Requiring $\phi_z\triangleq V_xg_x$, it follows that $z\triangleq c\delta/\tau$. For $V_z\triangleq V_xg_x$, the tip path plane angle $i\triangleq\tau$ or less.

For subsonic flow, it is assumed that $\delta\triangleq\tau$ and the linearized potential equation is obtained

$$(a_\infty^2\delta_{ij}-V_iV_j)\phi_{x_ix_j}=\phi_{tt}+2V_i\phi_{tx_i}+\dot{V}_i\phi_{x_i}$$

This equation can be simplified further for the rotor. For small tip path plane angles, all the V_z terms are higher order and the Ωx term in V_y can be neglected. Relative $a_\infty^2\phi_{xx}$, the $\dot{V}_i\phi_{x_i}$ terms are order c/R small. Relative $a_\infty^2\phi_{xx}$, ϕ_{tt} is order k^2 and $V_i\phi_{tx_i}$ is order k. So all of the unsteady terms must be retained if $k\triangleq 1$. For a once-per-revolution variation, $k\triangleq c/R$ is small and the equation is quasisteady. Hence, the equation for subsonic flow is

$$(a_\infty^2-V_x^2)\phi_{xx}-2V_xV_y\phi_{xy}+(a_\infty^2-V_y^2)\phi_{yy}+a_\infty^2\phi_{zz}$$
$$=\phi_{tt}+2V_x\phi_{tx}+2V_y\phi_{ty}$$

where the right-hand side is zero for frequencies $\omega\triangleq\Omega$. With transonic flow at the advancing tip, $M_x\cong 1$ or $V_x\cong a_\infty$ and the subsonic ordering assumptions are contradicted.

With transonic flow, it will be necessary to retain some of the nonlinear terms. For small disturbances, it is always possible to neglect the $\phi_{x_j}^2$ term in a^2, the order ϕ^3 terms, and the nonlinear unsteady terms. Thus,

$$\{[a_\infty^2-(\gamma-1)(\phi_t+V_i\phi_{x_i})]\delta_{ij}-V_iV_j-\phi_{x_i}V_j-V_i\phi_{x_j}\}\phi_{x_ix_j}$$
$$=\phi_{tt}+2V_i\phi_{tx_i}+\dot{V}_i\phi_{x_i}$$

Assume that the advancing tip Mach number is near 1, so $a_\infty^2-V_x^2\triangleq(\Omega R)^2\Delta$, for a small parameter Δ. Then, the nonlinear terms are required only for the coefficient of ϕ_{xx}. Requiring that the largest terms in the coefficient of ϕ_{xx} be the same order, $a_\infty^2-V_x^2\triangleq V_x\phi_x$, implies $\Delta\triangleq\delta$. For a nontrivial problem, the ϕ_{zz} term must be the same order as the ϕ_{xx} term, hence $\delta\triangleq\tau^{2/3}$ and $z\triangleq c/\tau^{1/3}$. For the problem to be three-dimensional, the ϕ_{yy} term must be of the same order as the ϕ_{xx} term, hence $y\triangleq c/\tau^{1/3}$. For yawed flow, the ϕ_{xy} term being the same order as the ϕ_{xx} term requires that the spanwise velocity be moderately small: $V_y\triangleq\Omega R\tau^{1/3}$. The remaining terms on the left-hand side are higher order (for small tip path plane incidence).

For unsteady flow, requiring that the ϕ_{tx} term be the same order as the ϕ_{xx} term implies $k\triangleq\tau^{2/3}$. For once-per-revolution time variation, $k\triangleq c/R$; so the problem is unsteady if $c/R\triangleq\tau^{2/3}$ and marginally unsteady if $c/R\triangleq\tau$. Alternatively, if it is assumed that $c/R\triangleq\tau$, it follows that the frequency must be $\omega/\Omega\triangleq\tau^{-1/3}$ for an unsteady problem.[63] If $k\triangleq 1$, the problem is more unsteady than transonic and the entire ordering scheme must change. The ϕ_t term (compared to $V_x\phi_x$) and the ϕ_{tt} term (compared to $V_x\phi_{tx}$) are order k small; nevertheless, they are sometimes retained to improve the rate of convergence of the solution.[64] The $\dot{V}_i\phi_{x_i}$ terms (compared to the ϕ_{xx} term) and Ωx in V_y or $\dot{V}_x$ are of order $\tau^{-1/3}c/R$. For $c/R\triangleq\tau$ these terms are of second order; but for $c/R\triangleq\tau^{2/3}$ (required for the problem to be unsteady with once-per-revolution time variation), they are only moderately small. In summary, the transonic scaling requires: $\phi/\Omega Rc\triangleq\tau^{2/3}$, $1-M_x^2\triangleq\tau^{2/3}$, $x\triangleq c$, y/c and $z/c\triangleq\tau^{-1/3}$, $M_y\triangleq\tau^{1/3}$, and $k\triangleq\tau^{2/3}$; exactly as for fixed-wing problems.

In the boundary condition, the V_z term must be retained for $i\triangleq\tau$, but $V_yg_y/V_xg_x=^\circ\tau^{2/3}$ and $g_t/V_xg_x=^\circ k$ are small. Hence, $\phi_z=V_xg_x-V_z$ on $z=0$. For small disturbances, the pressure may be approximated as

$$(p-p_\infty)/\rho_\infty\cong-(\phi_t+V_i\phi_{x_i}+\tfrac{1}{2}\phi_{x_i}\phi_{x_i})$$

which with the transonic scaling (as for a^2) becomes $(p-p_\infty)/\rho_\infty=-V_x\phi_x$.

The transonic domain is defined by $(1-M_x^2)\triangleq\tau^{2/3}$, where $V_x=\Omega y+\mu\Omega R\sin\psi$. The maximum Mach number $M_{at}=(1+\mu)\Omega R/a$ is at the advancing tip ($R=k$ and $\psi=90$ deg). Then for $M_{at}\cong 1$, the radial extent of transonic flow is $y/R\triangleq\tau^{2/3}$. So $c/R\triangleq\tau$ gives $y\triangleq c/\tau^{1/3}$, which is consistent with the differential equation being three-dimensional; for

$c/R = \tau^{2/3}$, the transonic domain is somewhat larger, $y \triangleq c$. The azimuthal extent of transonic flow is $\mu\psi^2 \triangleq \tau^{2/3}$, or $k \triangleq \mu^{1/2}\tau^{-1/3}c/R$. Then, $\mu \triangleq 1$ and $c/R \triangleq \tau$, or $\mu \triangleq \tau^{2/3}$ and $c/R \triangleq \tau^{2/3}$, give $k \triangleq \tau^{2/3}$, which is consistent with the equation being unsteady. For the transonic domain to be consistent with the equation being quasisteady ($k \triangleq \tau^{4/3}$) requires either a very small advance ratio or a very small c/R. Inside the transonic domain on the rotor tip, the radial velocity $V_y \equiv \mu\Omega R\cos\psi \triangleq \Omega R\mu^{1/2}\tau^{1/3}$, which is consistent with the requirement $V_y \triangleq \Omega R\tau^{1/3}$.

The transonic small-disturbance equation for potential flow on a rotary wing is thus,

$$(a_\infty^2 - V_x^2 - (\gamma+1)V_x\phi_x - (\gamma-1)\phi_t)\phi_{xx} - 2V_xV_y\phi_{xy} + a_\infty^2\phi_{yy} + a_\infty^2\phi_{zz} = \phi_{tt} + 2V_x\phi_{tx} + (2V_y\Omega + \Omega^2 x)\phi_x + (-2V_x\Omega + \Omega^2 y)\phi_y \quad (17)$$

which is nonlinear, unsteady, and three-dimensional. The $\dot{V}_i\phi_{x_i}$ terms on the right-hand side are almost higher order. Without them, the equation is identical to that for a fixed wing, except that V_x and V_y vary over the rotor disk. So the transonic nature dominates the equation of motion, while the effects of rotation enter through the variation of the wing velocities. The small-disturbance equations for the boundary condition and pressure are quasistatic and not affected by radial flow. A number of versions of Eq. (17) have been used, such as:

a) Without the $\dot{V}_i\phi_{x_i}$ terms; and neglect of Ωx in V_y in the ϕ_{xy} term.

b) Without the ϕ_{tt} and $\phi_t\phi_{xx}$ terms; without the $\dot{V}_i\phi_{x_i}$ terms; and neglect of Ωx in V_y in the ϕ_{xy} term.

c) Hover ($V_x = \Omega y$, $V_y = -\Omega x$); and steady.

d) Hover; steady; and without the $\dot{V}_i\phi_{x_i}$ and ϕ_{xy} terms.

Retaining all linear terms (i.e., unsteady and radial flow terms) in the boundary condition and pressure poses no difficulties.

The nonlinear equations were retained in Eq. (17) based on the assumption that the flow is in the x direction. In fact, a rotor blade has yawed flow, except exactly at $\psi = 90$ deg. Retaining the nonlinear terms for arbitrary yawed flow produces the following small-disturbance equation:

$$(a_\infty^2 - V_x^2 - (\gamma+1)V_x\phi_x - (\gamma-1)V_y\phi_y)\phi_{xx} + (a_\infty^2 - V_y^2 - (\gamma-1)V_x\phi_x - (\gamma+1)V_y\phi_y)\phi_{yy} + (a_\infty^2 - (\gamma-1)V_x\phi_x - (\gamma-1)V_y\phi_y)\phi_{zz} - 2(V_xV_y + V_x\phi_y + V_y\phi_x)\phi_{xy} = 2V_x\phi_{tx} + 2V_y\phi_{ty} + (2V_y\Omega + \Omega^2 x)\phi_x + (-2V_x\Omega + \Omega^2 y)\phi_y \quad (18)$$

Type-dependent differencing is applied in the direction of the local flow, at yaw angle $\Lambda = \tan^{-1}V_y/V_x$. Ignoring the variation of V_x and V_y with y and x, the second derivative in the local flow direction is $\phi_{ss} = C^2\phi_{xx} + 2CS\phi_{xy} + S^2\phi_{yy}$, where $C = \cos\Lambda$ and $S = \sin\Lambda$. Rearranging the left-hand side of Eq. (18) and retaining the nonlinear terms only in the coefficient of ϕ_{ss} gives

$$[a_\infty^2 - (V_x^2 + V_y^2) - (\gamma+1)(V_x\phi_x + V_y\phi_y)] \times (C^2\phi_{xx} + 2CS\phi_{xy} + S^2\phi_{yy}) + a_\infty^2(S^2\phi_{xx} - 2CS\phi_{xy} + C^2\phi_{yy} + \phi_{zz}) = 2V_x\phi_{tx} + 2V_y\phi_{ty} + (2V_y\Omega + \Omega^2 x)\phi_x + (-2V_x\Omega + \Omega^2 y)\phi_y \quad (19)$$

When using Eq. (18) or (19), the radial flow terms are retained in the boundary condition and pressure as well.

The transonic equation for a rotor has generally been solved by a finite difference method adapted from fixed-wing research. The type-dependent differencing of Murman and Cole[65] is used for the x derivative (central differencing in subsonic flow, backward differencing in supersonic flow). The type-dependent differencing is in the local flow direction

Table 3 Rotary wing transonic theory

Ref.	Eq.	Hover/steady, quasisteady, or unsteady	Lifting or nonlifting	Comments
			Small disturbance	
63	17b	U	N	—
66	17c	HS	N	—
67	17c	HS	N	—
68	17d	HS	L	Preceding blade tip vortex
64	17a	U	N	—
69	—	U	L	Two-dimensional
70	17a	U	N	—
71	17b	U	N	—
72,73	17b	U	N	—
74	17b	U	L	Preceding blade tip vortex
75	17b	U	L	Coupled with wake (CAMRAD)
76	17b	U	L	Oblique wake
76	19	U	N	—
77-79	18	QS	L	Oblique wake
80,81	—	U	L	Two-dimensional
80,81	—	QS	L	Finite element
			Full potential	
82-84	16	QS	L	ROT22
85	16	HS	L	—
86	16	QS	L	TFAR1
86	16	U	L	TFAR2
87	16	QS	L	Coupled with wake (CAMRAD); curved wake
88	16	U	L	Coupled with wake (CAMRAD)
89	—	US	L	RFS2; coupled with wake (CAMRAD)

for full potential methods and in some of the small-disturbance methods as well. For a swept blade, the tip planform is transformed to a rectangle before generating the computation grid; a body-fitted grid is required for full potential methods. The small-disturbance equation can be solved faster than the full potential or Euler equations, but the former is not valid for angles of attack above about 5 deg and never at the leading edge. To reduce the computation time, the quasistatic equations can be solved; all of the time derivatives in the potential equation are neglected, although the correct instantaneous velocities and boundary conditions are used. To define the loading on the advancing blade tip, the unsteady equation must be solved at many more azimuth locations than is necessary with the quasistatic equation.

Most often the far-field boundary condition of $\phi = 0$ has been used and two-dimensional flow (all y derivatives zero) is required on the inboard face if the computational domain does not include the entire blade. For unsteady solutions, the analysis is started in the subsonic region, where the problem is quasistatic. The wake behind a lifting blade is a planar surface, with a potential jump $\Delta\phi$ convected downstream from the trailing edge. The curvature of the wake has almost always been neglected. In some cases, a tip vortex from a preceding blade has been included in the finite difference computation domain, as a potential jump on a branch cut. The more general problem of coupling the transonic analysis with a complete rotor wake and blade motion solution has been attempted so far using lifting line concepts: the influence of the blade motion and wake (outside the computation domain) is included as an angle of attack in the wing boundary condition; then the lift calculated by the transonic analysis is used in solving for the blade motion and wake-induced velocity.

Literature

Table 3 sumarizes the work that has been done with transonic analyses of rotors. [63,64,66-89] Caradonna[70] and Tung et al.[75] retained Ωx in V_y in the ϕ_{xy} term. Desopper[76] included the ϕ_{tt} term and introduced some additional approximations during the coordinate transformation for a swept tip. Arieli and Tauber[82,83] used a rotating, but not translating, coordinate frame, with a quasisteady freestream relative to the rotating blade; as a result, part of the $\dot{V}_i\phi_{x_i}$ terms were omitted in the quasistatic approximation. Sankar and Prichard[89] solved the full potential equations in conservation form (except for the time derivatives). Wake et al.[90] solved the unsteady Euler equations for the flow about a nonlifting rotor blade.

The calculations and comparison with experiment have demonstrated the fundamental unsteady[64,69-73,82-84,86,89] and three-dimensional[64,69,80,81,86] nature of transonic flow on the advancing blade tip. Radial flow is also important.[78] Figure 6 compares the unsteady and quasisteady calculations with the pressure measurements. Figures 7-9 compare transonic calculations with ONERA measurements of the pressures on a nonlifting, rectangular tip rotor blade in forward flight.[69,72,73] A similar comparison was made by Chattot and Philippe.[72,73] For a swept blade, Chattot and Philippe[72] found too rapid a disappearance of the shock in the second quadrant. So Desopper[76] used Eq. (19) to retain more influence of the radial flow and obtained a better correlation with experiment (Fig. 10). Using Eq. (19) also improved the stability of the calculations, so an azimuth increment of 1 deg could be used (just as for a rectangular tip), instead of ⅛ deg with version b of Eq. (17). Transonic analyses have been used to design swept tips for rotor blades.[72,73,79] Tests have shown improved rotor performance in high-speed forward flight with swept tips,[76] which the theory attributed to a decrease in the transonic flow intensity for azimuth angles up to 130 deg (there was a slight increase from 140 to 150 deg).

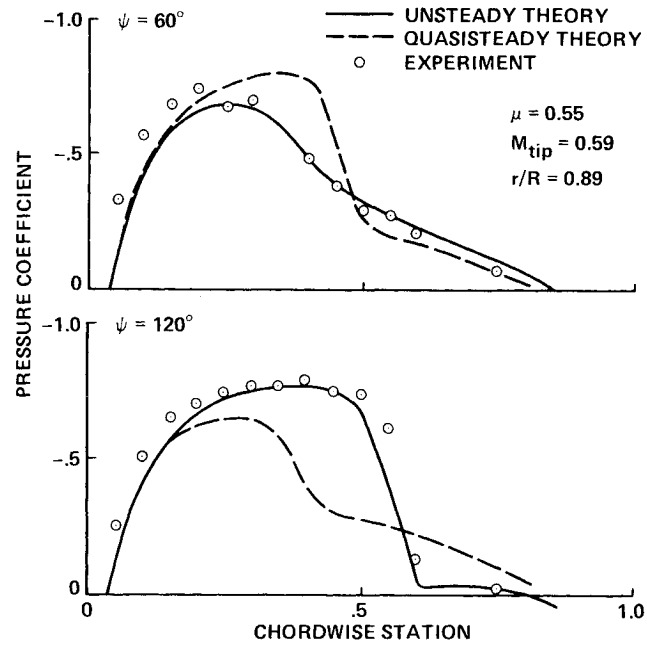

Fig. 6 Transonic flow on nonlifting rotor blade, small-disturbance calculations.[72]

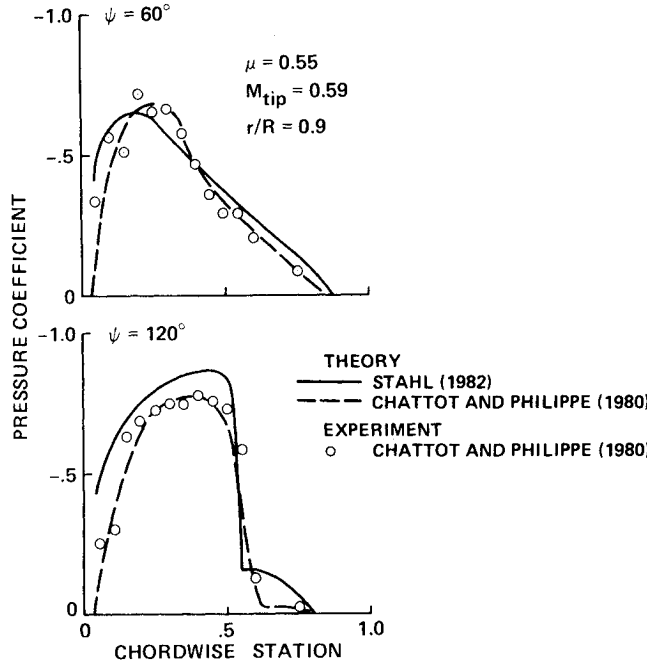

Fig. 7 Transonic flow on nonlifting rotor blade, small-disturbance calculations.[72,80]

Comparisons with nonlifting data have the advantage that only the transonic flow features need be considered; however, in lifting rotor flows, the wake and blade motion are important. A practical method to account for the rotor wake is required, even though it is now possible with finite difference methods to only calculate the flowfield near the blade. A preceding blade tip vortex can be included in the finite difference calculation,[68,74] but the primary approach used so far involves coupling with the wake through the boundary condition at the blade. The transonic flow can be calculated for a prescribed angle-of-attack distribution obtained from the blade motion and uniform inflow.[69,74,76-78] Several of the transonic rotor theories have been coupled with a comprehensive helicopter analysis[91] that calculated

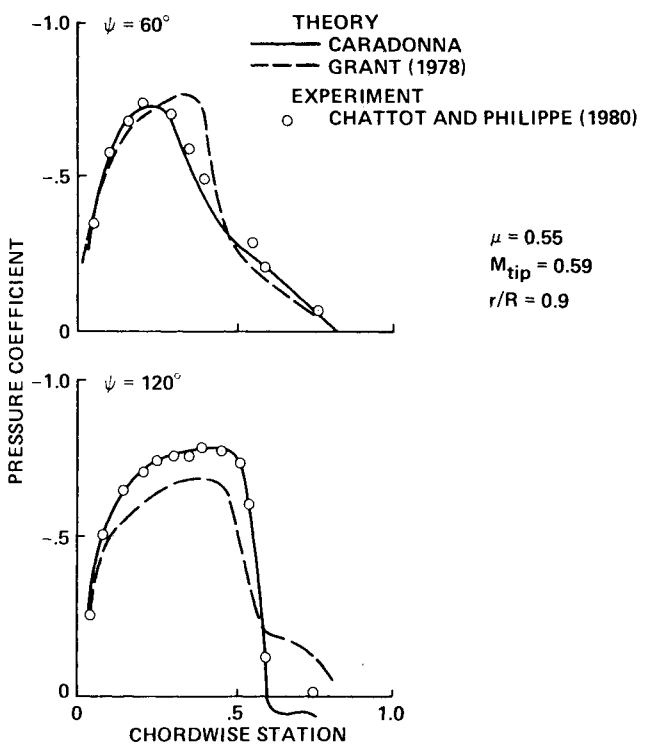

Fig. 8 Transonic flow on nonlifting rotor blade, small-disturbance calculations.[72,78]

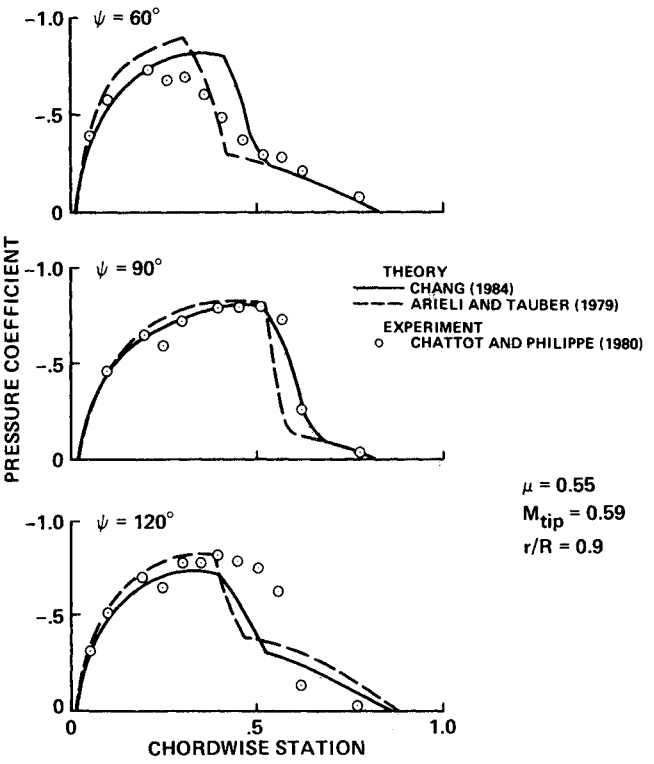

Fig. 9 Transonic flow on nonlifting rotor blade, quasistatic full potential calculations.[82,86]

the rotor wake and blade motion, for a complete forward flight analysis. The helicopter analysis (CAMRAD) calculated an angle-of-attack distribution, excluding the blade near wake that was included in the finite difference domain; the finite difference code used this angle of attack to calculate the blade lift on the advancing side; and then CAMRAD used the finite difference lift, plus a lift increment produced by the update of the wake and blade motion. These steps were repeated until the finite difference lift calculation converged. The method was consistent and efficient, with fast convergence: usually only two executions of the finite difference code were required. Figure 11 compares measured forward flight pressure data[92] with such calculations using three transonic theories. The small-disturbance theory[71,75] underpredicted the leading-edge pressure in the first quadrant; the calculated angle of attack is about 6 deg at $\psi = 0$. The quasisteady, full potential theory[86,87] gave better results in the first quadrant, but worse in the second quadrant. The unsteady, full potential theory[86,88] unexpectedly predicted too strong a shock at $\psi = 120$ deg.

Wake Analysis

The vortex wake is an important, and often crucial, element in all helicopter problems, including performance, structural loads and vibration, stability, and noise. The manner in which complete wake models are to be incorporated into advanced computational techniques has not been fully established. Current helicopter performance and loads analyses[1] use a wake model consisting of a finite core line for the tip vortex, typically as a connected series of straight line segments; a vortex lattice for the inboard trailed and shed vortex sheet; and perhaps some model of the roll-up process. Forward flight free-wake geometry calculations (such as Ref. 93) are well developed, but the early methods for hover wake geometry calculation (e.g., Refs. 94 and 95) were not satisfactory. The current standard approach for hover calculations is to use a prescribed wake geometry model, based on model rotor flow visualization.

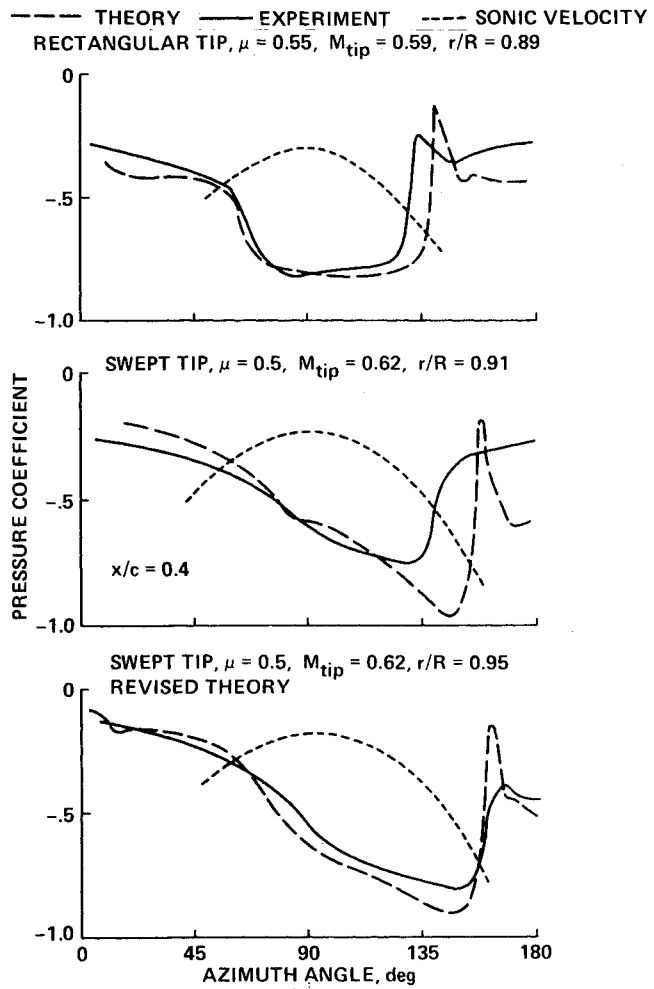

Fig. 10 Transonic flow on nonlifting rotor blade, small-disturbance calculations.[72,76]

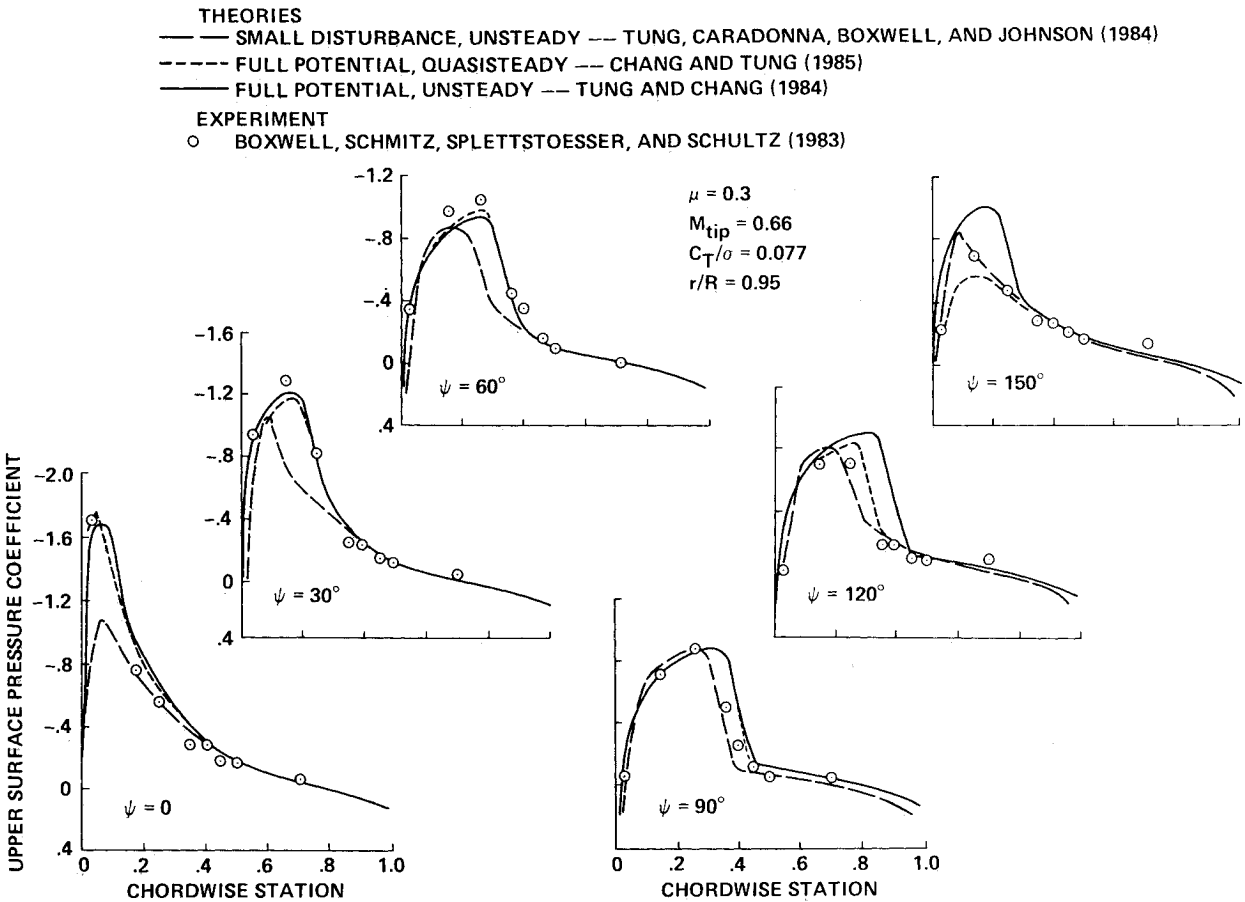

Fig. 11 Transonic flow calculations on lifting rotor blade, coupled with rotor wake and blade motion calculations.[75,87,88]

Hovering Rotor Wake Models

A number of the panel method solutions for the hovering rotor include a free-wake geometry calculation.[26,53,54,56,57] The wake models in these methods are not new, but they are a consistent part of the solution for the three-dimensional wing loading. Discretized vortex singularity models of the wake, either with lifting line or panel wing theories, are perhaps sufficient to describe the overall behavior. More sophisticated models are required to calculate the detailed behavior, such as the tip vortex formation and roll-up.

Miller[96] developed a hover free-wake geometry calculation, using two-dimensional and axisymmetric (ring) models for efficiency. The wake was assumed to have rolled up into three vortices (tip, inboard, and root), replaced by a far-wake model after four revolutions. The average velocity between the vortices was used to determine the wake geometry. Murman and Stremel[97] calculated two-dimensional unsteady wake development by a cloud-in-cell method (which would be more efficient than a direct application of Biot-Savart equation). Discrete vortex elements in the wake were tracked in a Lagrangian frame. For each time step, the vorticity was distributed to a fixed (Eulerian) mesh, on which the velocities were calculated by a finite difference solution of Laplace's equation (with potential jumps on branch cuts to represent the vorticity). Next, the velocity was interpolated to the vortex positions, which were then integrated to the next time step. The distribution of vorticity to the Eulerian mesh introduced an effective core radius, on the order of the grid size, that eliminated the velocity singularities (vortex tracking methods are unstable with point vortices). Yet there was no diffusion of vorticity (artificial viscosity), since the vortex elements were tracked individually. Stremel[98] applied this two-dimensional model to hovering rotor wake roll-up. He used three vortices (tip, inboard, and root) for five revolutions, plus intermediate and far-wake models, to represent the rotor wake. Stremel[99] developed a method to separate the grid size from the viscous core size in the cloud-in-cell method, which is desirable whether the core is intended to be a physical model or simply to control the numerical instabilities. In particular, the capability to use a small core radius with a large mesh size is needed for efficiency. In the solution for the velocities, the finite difference approximation for the derivatives of the vorticity distribution was the source of the effective core radius and of errors for small core size. A correction was introduced for close vortices such that the solution of the finite difference equations for the velocity would be exact. A significant influence of the core size on the tip vortex roll-up was calculated (Fig. 12).

Roberts[100] developed a cloud-in-cell method to calculate hovering rotor wake geometry, using an axisymmetric (ring) model. The ring vortex self-induced velocity was found to be grid dependent (an effective core radius). This effect was eliminated by calculating the self-induced velocity of each ring exactly, using the true core radius; the cloud-in-cell method accounted for the influence of the other rings. The rotor wake geometry calculations converged using 2-10 vortex elements radially, but did not converge using 20-40 elements, except with a coarse grid. Roberts and Murman[101] coupled this wake geometry model with a lifting line theory calculation of the blade loading. The results were very close to Miller's two-dimensional calculations; agreement with experiment was fair.

Liu et al.[102] solved the incompressible, laminar, Navier-Stokes equations for a hovering rotor wake. They used an unsteady, axisymmetric (ring) model of the wake. The vorticity distribution at the blade trailing edge, from a separate lifting surface calculation of the blade loading, was intro-

duced at the blade passage frequency, with the vertical separation from a prescribed wake model. The computation domain included nine revolutions, with no far-wake model. The calculations showed little wake contraction and significant vortex diffusion (the Reynolds number, based on the rotor radius, was only 40,000). Cantaloube and Huberson[103] developed a unique representation of the rotor wake for both hover and forward flight, in terms of vortex-carrying particles emitted at the blade trailing edge. The blade loads were calculated using incompressible lifting surface theory for a thin wing. Cantaloube[104] applied the method to isolated rotor and rotor/body configurations.

Egolf and Sparks[105] coupled a full potential solution for the near field of a hovering rotor blade with an incompressible, discrete vortex solution for the far field. The wake geometry was prescribed, hence the far-field solution determined the velocity potential on the boundaries of the finite difference computational domain. The full potential solution included the trailed wake and any tip vortices from preceding blades that were in the computational domain. Roberts and Murman[106] solved the three-dimensional, steady Euler equations for the near field of a hovering rotor blade, including the tip vortex formation. The tip vortices in the computation domain below the blade had strength and position defined by a free-wake geometry calculation.[100] The velocity was split into a wake-induced component (known) and a remainder (produced by the vorticity of the blade and the shocks). The solution for the remainder was found such that the total velocity field satisfied the Euler equations. This approach eliminated the numerical diffusion of the wake vorticity (solutions with the wake defined by boundary conditions on the computation domain were similar to the results obtained by omitting the wake entirely). Moreover, the remainder velocity component was smooth away from the rotor, since the primary contribution of the returning wake was already accounted for. A far-wake model was used, giving an induced-velocity boundary condition at the outer boundary. Sankar et al.[107] solved the three-dimensional, unsteady Euler equations for a hovering rotor tip. The wake-induced velocity for a helical tip vortex was calculated using the Biot-Savart equation and then the remaining velocity component was found, such that the total satisfied the Euler equations.

Transonic Blade/Vortex Interaction

Table 4 summarizes the work that has been done to analyze the transonic interaction of a blade and its vortex.[68,70,74,101-116] The two-dimensional interaction is an idealized model of phenomena that can be encountered in rotor flowfields. The analyses have been conducted for Mach numbers of 0.8-0.85, although the two-dimensional encounter on a helicopter rotor would be at a lower Mach number. The high Mach number blade/vortex interaction problem is really three-dimensional. Moreover, viscous effects are often significant for blade/vortex interaction on helicopter rotors. The two-dimensional transonic investigations are laying the foundation for ways to include wake vorticity in the finite difference rotor analyses.

The small disturbance code LTRAN2-HI of Ballhaus and Goorjian[117] was the basis for several of the analyses[109-111] in Table 4. George and Chang[110] encountered numerical problems with a concentrated vortex, because of shifting branch cuts between mesh points as the vortex moved and the large velocities near the point vortex. The problem was eliminated by using a vortex core, with the vorticity distributed to the

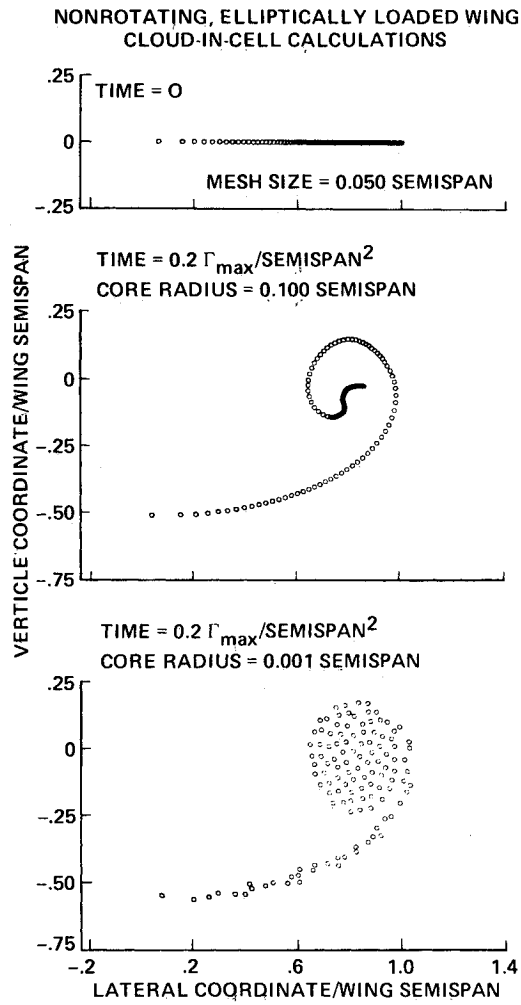

Fig. 12 Vortex wake development for elliptically loaded wing, cloud-in-cell calculations.[99]

Table 4 Transonic blade-vortex interaction analyses

Ref.	Eq.	Vortex path	Vortex boundary conditions
		Three-dimensional steady—perpendicular	
68	SDP[a]	Prescribed	Potential jump on branch cut
74	SDP	Prescribed	Potential jump on branch cut
108	Euler	Free	Velocity and pressure on upstream boundary
		Two-dimensional unsteady—parallel	
70	SDP	Prescribed	Potential jump on branch cut
109	SDP	Prescribed	Vortex-induced vertical velocity at airfoil
110	SDP	Free	Vortex-in-cell with multiple branch cuts
111	SDP	Free	Vortex-induced velocity added to flowfield
112-114	Euler and Navier-Stokes	Prescribed	Prescribed vortex-induced flowfield
115,116	Euler	Free	Upstream initial conditions of velocity

[a]Small disturbance potential equation.

grid points at each time step. The core was square, was not distorted by the interaction, and had a size equal to 25% of the chord (to avoid a supersonic region around the vortex). McCroskey and Goorjian[111] used a 5% chord vortex core radius to eliminate a numerical instability caused by the streamwise velocity component. Srinivasan et al.[112] solved the thin-layer Navier-Stokes equations for high Reynolds number turbulent flow. They solved for the perturbation flow about the inviscid (Euler) solution for the vortex in a freestream (without the airfoil). With this method, the far grid could remain coarse, since the vortex flow had already been accounted for. When the vortex was specified as an upstream initial condition,[113] numerical dissipation with a reasonable grid greatly reduced the vorticity concentration. Sankar and Tang[115] solved the compressible Navier-Stokes equations for turbulent flow. Smoothing the total flowfield (artificial dissipation) was found to introduce significant diffusion of the vorticity, especially with a coarse grid upstream; when smoothing was applied only to the difference between the flowfield and that of an isolated vortex, excessive numerical diffusion was avoided. In this method, the force-free vortex path was obtained. They also considered a prescribed vortex path analysis, with nonlinear superposition of the vortex flowfield (as in Ref. 112).

The calculations show a significant influence of the vortex on the shock position and strength. There is a significant effect of unsteadiness: with a convected rather than a fixed vortex the interaction is much reduced.[70,112] A free rather than a prescribed vortex path produces only a small change in the interaction.[111,113] Figures 13 and 14 compare the airfoil loads calculated by several of the methods[112,115] (other comparisons are given in Refs. 110 and 111). The three codes in Fig. 13 produced qualitatively similar results. There was little influence of viscosity in the calculations, either with or without the vortex; and the vortex-induced effects were generally within the scope of the small disturbance approximation, except for a tendency to overpredict the interaction effects at the leading edge of a thin airfoil.[112,116] Small-disturbance calculations are less accurate and less stable for either very strong or very close vortices.[113] A linear analysis gave about the same results for the lift and moment coefficients, although the pressure distributions were of course very different.[111] The differences in Fig. 14 reflect the influence not of the vortex path, but rather of the method used to represent the vortex.

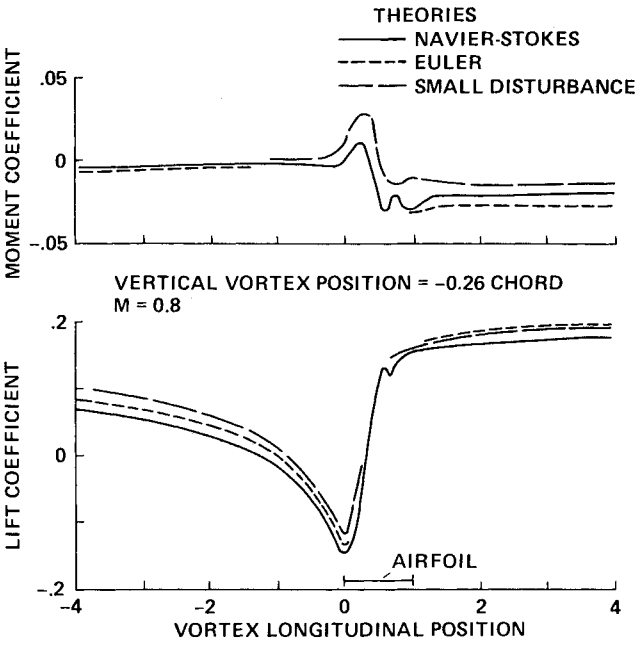

Fig. 13 Two-dimensional transonic blade/vortex interaction.[112]

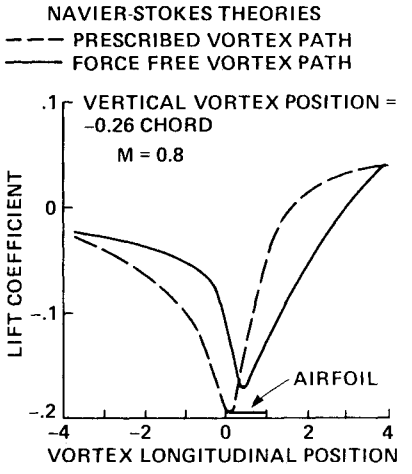

Fig. 14 Two-dimensional transonic blade/vortex interaction.[115]

Limitations of Computational Aerodynamics

The factors that currently limit advanced aerodynamic computations have been often enumerated: computer speed and memory, algorithm and solution methods, grid generation, vortex modeling, and turbulence modeling. Even in steady forward flight, the aerodynamics of a helicopter are unsteady and compressible, with significant wake effects and complex geometry, and are coupled with the system structural dynamics. Hence, analyses that are limited to steady or incompressible motion, simple wake models, simple grids, and just the aerodynamic forces are less useful than for fixed-wing aircraft.

Turbulence modeling limits the physical representation of the flows.[118] As long as resolution of the turbulence scales at large Reynolds number is impractical, it is necessary to use turbulence models for closure of the Reynolds-averaged Navier-Stokes equations. No universal turbulence model, applicable to a wide variety of flows, has been found. Thus, a catalog of models based on fundamental expriments must be developed and the capabilities and limitations of each model established by extensive correlation between the calculations and measurements. Moreover, the most complex turbulence models (multiple-equation eddy-viscosity and Reynolds-stress equation models) are generally used for steady problems; unsteady calculations have used simpler models (such as a zero-equation eddy-viscosity model).

The fact that the maximum time step required for stability is much less than that for accuracy is a major limitation of Euler and Navier-Stokes calculations.[119] The requirement for algorithms that relax the stability limitation on the time step is particularly important for helicopter problems, which are very often unsteady. The great influence of the wake in helicopter problems means that accurate vortex models are essential. Moreover, when the wake is included, the computational domain has dimensions on the order of the rotor diameter, not the blade chord (as would be appropriate if only the flow near the wing were needed). Regarding grid generation, the helicopter problem introduces the need to eventually interface rotating and nonrotating components.[119] Rotor blades vibrate, even in steady forward flight. The task of coupling advanced aerodynamic and structural dynamic calculations for helicopters has not yet been given much attention. Calculations restricted to the aerodynamic side of rotor behavior have limited applications.

The practicality of an analysis method can be expressed in terms of computation time, which is determined by algorithm and machine capabilities. Computation times naturally increase with the complexity of the model. For current three-dimensional unsteady calculations,[118] full potential

methods take about 3 times longer than small-disturbance methods; Euler methods about 20 times longer than full potential; and Navier-Stokes methods about 50 times longer than Euler. Fortunately, the prospects for reducing times are greater for the more complex methods[118]; a factor of 10 reduction should be possible for full potential methods and a factor of 100 for Navier-Stokes methods. The use of solution-adaptive grids should reduce the number of computation points required. It should be possible to increase the maximum time step by a factor of 10 or 20 using improved implicit algorithms (to remove the stability limit). What computations are practical now is illustrated by the recent research cited in this paper. Two-dimensional Navier-Stokes and three-dimensional Euler calculations (with limited computational domains) are being performed.

The goal is to perform viscous computations for the entire rotor and airframe—one of the most demanding problems being considered in computational aerodynamics. McCroskey and Baeder[119] have estimated the computation requirements for this problem: 4000 h/MFLOP (million floating-point operations per second) and 30×10^6 words of memory. They considered two revolutions of a relatively simple rotor and fuselage, a thin-layer Navier-Stokes method with an algebraic eddy-viscosity turbulence model and a solution algorithm allowing a time step determined by accuracy (not stability). Hence, this estimate is the minimum for the helicopter problem and perhaps somewhat optimistic. The High-Speed Processor-1 (HSP-1, operational in 1986) of NASA's Numerical Aerodynamic Simulation (NAS) program has a compute speed for optimized large-scale calculations of 250 MFLOP and 256×10^6 words of central memory. The memory is sufficient for the helicopter problem, but the NAS HSP-1 speed implies a computation time of 16 h. The NAS HSP-2 has a goal of 1000 MFLOP and 1000×10^6 words of memory, which would reduce the time to about 4 h. These times are long, but are acceptable for initial research. Thus, Navier-Stokes calculations for a complete rotorcraft are worth initiating, although they will be beyond the reach of routine applications for some time.

Viscous Flow Methods

Dynamic Stall Theories

Dynamic stall is a flow phenomenon of rotor blades that involves large-scale, unsteady viscous effects. The incompressible case is of interest, but the effects of compressibility are significant. Although the yawed flow on a rotor blade does have an influence, the fundamental behavior is contained in the two-dimensional problem. The work of McCroskey (particularly Refs. 120 and 121) provides a description of dynamic stall and reviews of the experimental and theoretical research.

For an airfoil oscillating in pitch, a rapid increase in angle of attack can delay stall. When dynamic stall does occur, it is more severe and more persistent than static stall, with a large amount of hysteresis. The character of dynamic stall is determined primarily by the maximum angle of attack during the oscillation, with four regimes identifiable.[121] In the no-stall regime, the viscous/inviscid interaction is weak, and the vertical scale of the viscous zone is of the order of the boundary-layer thickness. For an NACA 0012 airfoil, this regime extends up to $\alpha_{max} = 13$ deg (for low Mach number). In this regime, there is little separation and the viscous effects are small. In the stall onset regime (around $\alpha_{max} = 14$ deg for an NACA 0012 airfoil), there is some separation during part of the oscillation cycle. This regime gives the maximum lift possible with no significant penalty on section moment or drag. In the light stall regime (around $\alpha_{max} = 15$ deg

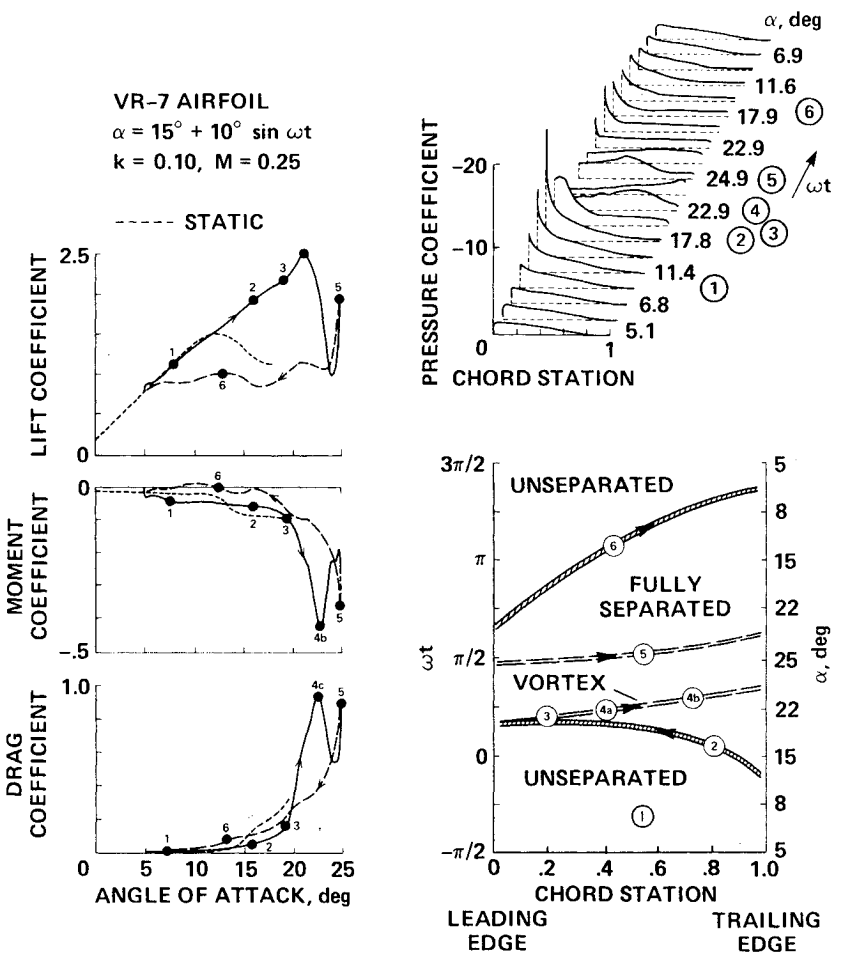

Fig. 15 Dynamic stall events on an oscillating airfoil.[120]

for an NACA 0012 airfoil), the viscous/inviscid interaction is strong and the vertical scale of the viscous zone is of the order of the airfoil thickness. The airfoil loads show the usual static stall effects, plus phase lags and hysteresis. The tendency for negative pitch damping is strongest in this regime. The loads are most sensitive to the airfoil geometry, pitch rate, maximum angle of attack, and Mach number in this regime. In the deep stall regime (around $\alpha_{max} = 20$ deg for an NACA 0012 airfoil), the flow is dominated by viscosity, with the vertical scale of the viscous zone on the order of the airfoil chord. The viscous zone exists over the upper surface during most of the cycle. The flow is characterized by shedding of a large vortex-like disturbance from the leading edge, which passes over the upper surface and produces section loads far in excess of the static values while the angle of attack is increasing, and a large amount of hysteresis.

Figure 15 illustrates the dynamic stall events on an oscillating airfoil.[120] Point 1 is in the unseparated domain, with a thin, attached boundary layer. The section loads behave as predicted by linear, unsteady theory. At point 2, above the static stall angle, flow reversal within the boundary layer develops, but the lift continues to increase, extrapolated from the linear domain. For airfoils exhibiting trailing-edge stall (as in Fig. 15), the reversed flow starts at the trailing edge and moves forward. For airfoils exhibiting leading-edge stall, the reversed flow develops quickly and very locally just downstream of the suction peak on the upper surface. At point 3, for both types of airfoil, a vortex begins to evolve near the leading edge and spreads rearward over the upper surface (at about half the freestream velocity), distorting the pressure distribution. The pitching moment diverges and the drag begins to rise; but the lift is still increasing as a result of the vortex. At point 4, with the vortex near the trailing edge, the maximum lift, drag, and moment occur (not simultaneously), followed by rapid drops. Secondary vortices may be shed, producing further load fluctuations (point 5). At point 6, the angle of attack is decreasing, with large hysteresis as the reattached flow develops from the leading edge.

Empirical models are currently the only practical means to include the effects of dynamic stall in helicopter flow calculations. McCroskey[120,122] reviews the early models. The present trend is to develop finite state differential equation models for the section loads, based on measured static data. Dynamic stall theories are needed, initially to support and ultimately to replace such empirical models. The advanced computation methods being applied to dynamic stall may be classed as vortex theories and Navier-Stokes calculations. In vortex theories,[123-127] point vortices are shed from the airfoil and tracked in the flowfield (generally using the Biot-Savart equation). Vortex methods readily predict the effects of the leading-edge vortex, but the viscous aspects of the problem are prescribed, modeled, or approximated. Ham[123] allowed vortices to be shed from the leading and trailing edges of a flat-plate airfoil, with the strength determined by the requirement that the leading and trailing edges be stagnation points; the time that the shedding started was prescribed. Baudu et al.[124] allowed vortex shedding from the separation point (calculated by a boundary-layer analysis), with the strength determined by the boundary-layer vorticity; the starting time and initial direction of the shedding were prescribed. Spalart et al.[126,127] allowed vortex shedding aft of the separation point (calculated by a steady boundary-layer analysis), with the strength determined by the airfoil surface vorticity. Panel methods have also been applied to the dynamic stall problem.[45,46,128,129] Maskew and Dvorak[45] developed a panel method for static stall of an airfoil with trailing-edge separation. The free shear layer of the wake boundary was modeled by a vortex sheet, with the constant strength determined by the airfoil vorticity at separation. The wake boundary was required to be a streamline. A boundary-layer calculation gave the separation point. Rao et al.[128] used this

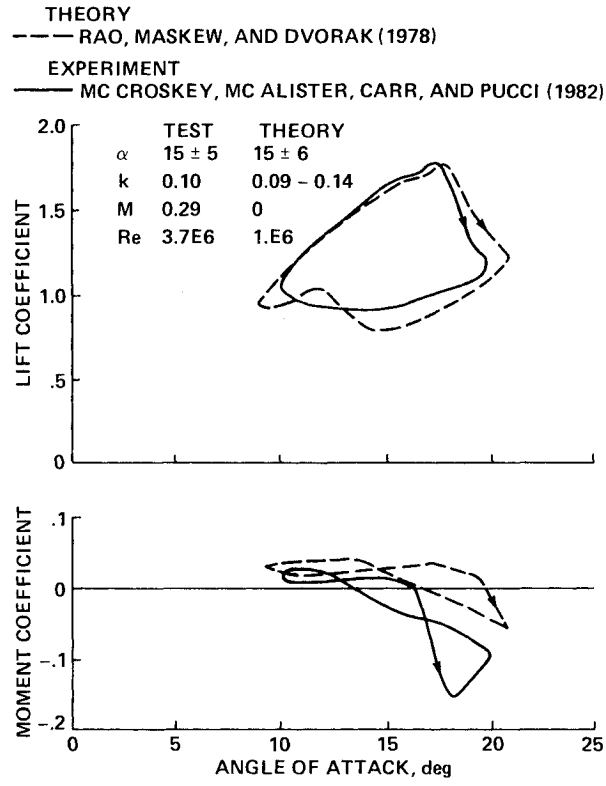

Fig. 16 Panel method calculations of two-dimensional dynamic stall loads.[128]

static analysis (at an angle of attack with a constant phase lag) to determine the wake model for an unsteady panel code, producing a method for dynamic stall with trailing-edge separation but no leading-edge vortex. Maskew and Dvorak[129] began the extension of the static analysis to include a time-dependent free wake. The vortex sheets modeling separation had time-varying strength and were allowed to distort and roll up; the model was intended to include the leading-edge vortex. In preliminary calculations, the location and time that separation started were prescribed rather than calculated.

Navier-Stokes calculations of dynamic stall are still expensive, but are beginning to be effective. Calculations have not yet been attempted for cases with extreme influence of the leading-edge vortex. Finite difference methods are used to solve the unsteady Navier-Stokes equations, usually for compressible flow. Mehta[130] considered incompressible, laminar (low Reynolds number) flow; the calculations showed the leading-edge vortex shedding, qualitatively similar to experiment. Shamroth and Gibeling[131] considered turbulent flow for a ramp change in angle of attack; the rate of change was not high enough to produce a leading-edge vortex. Sankar and Tassa[132] calculated dynamic stall for laminar flow. Tassa and Sankar[133] and Sankar and Tang[115] solved the compressible, unsteady Navier-Stokes equations for turbulent flow on an oscillating airfoil.

Figures 16-20 compare dynamic stall calculations from several methods with the lift and moment measured on an NACA 0012 airfoil oscillating in pitch.[134] All of these cases, with $\alpha_{max} = 20$ or 25 deg, are in the deep dynamic stall regime.[121] However, the experimental data for Fig. 16 show very little influence of the leading-edge vortex, so the case is consistent with the theory for unsteady trailing-edge separation.[128] The leading-edge vortex influence is evident in the experimental data for Figs. 17-20, although they do not represent the most extreme cases possible. Intending to simulate the influence of transition, Sankar and Tang[115] used a Reynolds number of 1.0×10^6 in the calculations, rather

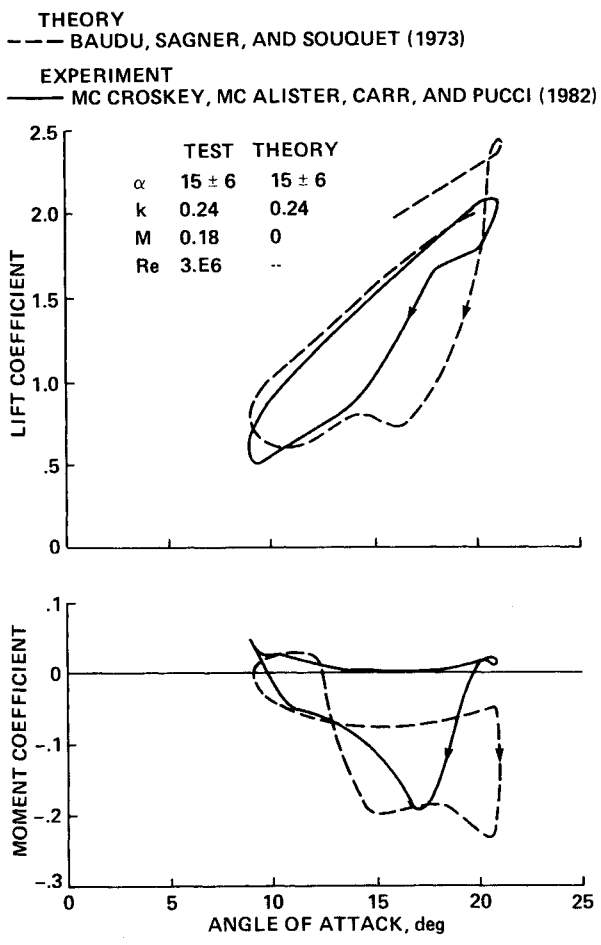

Fig. 17 Vortex method calculations of two-dimensional dynamic stall loads.[124]

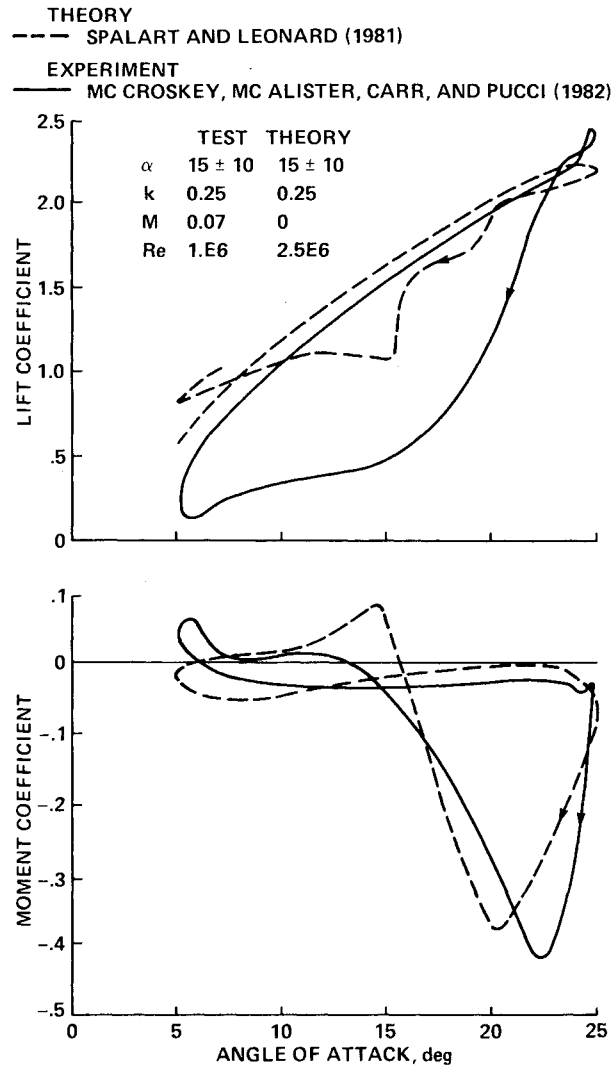

Fig. 18 Vortex method calculations of two-dimensional dynamic stall loads.[126]

than the 3.5×10^6 of the experiment (Fig. 20). The experimental data show less influence of the leading-edge vortex for a Reynolds number of 1.0×10^6 (or even 2.4×10^6), with lift and moment stall occurring at maximum angle of attack. The error in Fig. 20 was attributed to the turbulence model, motion of the transition point, and grid resolution.

Lifting Line Theory

Lifting line theory remains the only computationally effective method for the general calculation of helicopter air loads including the effects of viscosity. Even in normal forward-flight operating conditions, the rotor blade stalls on some part of the disk and significant stall occurs before the integrated rotor performance degrades. So it is essential that a useful helicopter aerodynamic theory include stall. Lifting line theory allows the combination of three-dimensional influences (the wake) with two-dimensional solutions that include the stall and compressibility effects. Lifting line concepts are also often invoked when implementing advanced methods: in panel methods and lifting surface theory, lifting line theory can be the basis for correcting the lift for stall and compressibility and evaluating the profile drag[52,135]; and lifting line theory can be the basis for coupling transonic tip finite difference calculations with a global wake and blade motion solution.[75,87,88]

A practical implementation of lifting line theory in rotor analyses—or at least as practiced—takes the following form. The outer problem consists of an incompressible vortex wake from a bound vortex at the quarter chord, perhaps with distorted geometry. The induced velocity (three components, constant over the chord) is evaluated at the three-quarter chord point, excluding the bound vortex (and perhaps excluding the inner shed wake as well). The inner problem consists of unsteady, compressible Navier-Stokes equations for an infinite-aspect-ratio, yawed wing in a uniform freestream produced by the rotation and translation of the wing, plus the wake-induced velocities. Normally, the inner problem is split into the two-dimensional, steady, compressible Navier-Stokes equations (airfoil tables), plus corrections for unsteady flow (small angle, perhaps including the inner shed wake), dynamic stall, and yawed flow. It is useful to examine the derivation of lifting line theory to see what must be assumed for this implementation to be valid.

Examination of the theory shows, and experience confirms, that this implementation of lifting line theory is almost second-order accurate for the lift. It is only first-order accurate for the moment, which is not very satisfactory for three-dimensional effects, but is acceptable when two-dimensional effects (such as dynamic stall) are dominant. For a steady, incompressible, nonrotating wing, this theory is equivalent to Weissinger's L-method for tapered and swept wings. Weissinger[136] found the L-method to be as accurate as a simplified lifting surface theory. DeYoung and Harper[137] showed that the L-method gave good predictions of measured span loading for wings with a wide range of aspect ratio, sweep, and taper. Brower[138] compared vortex lattice lifting surface theory, Prandtl's (first-order) lifting line theory, and Weissinger's lifting line theory for nonrotating blade/vortex interaction. The L-method gave excellent results even for very small blade/vortex separation.

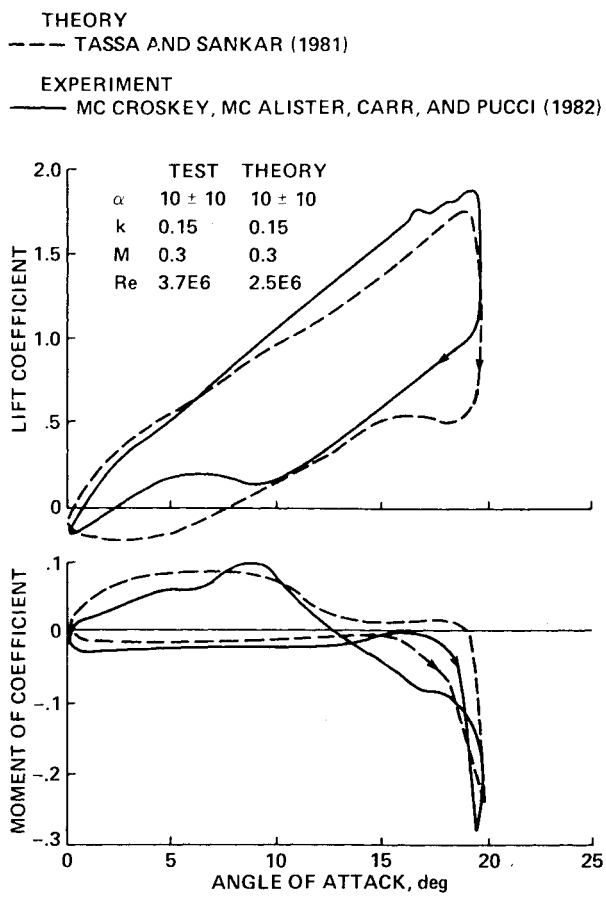

Fig. 19 Compressible, turbulent Navier-Stokes calculations of two-dimensional dynamic stall loads.[133]

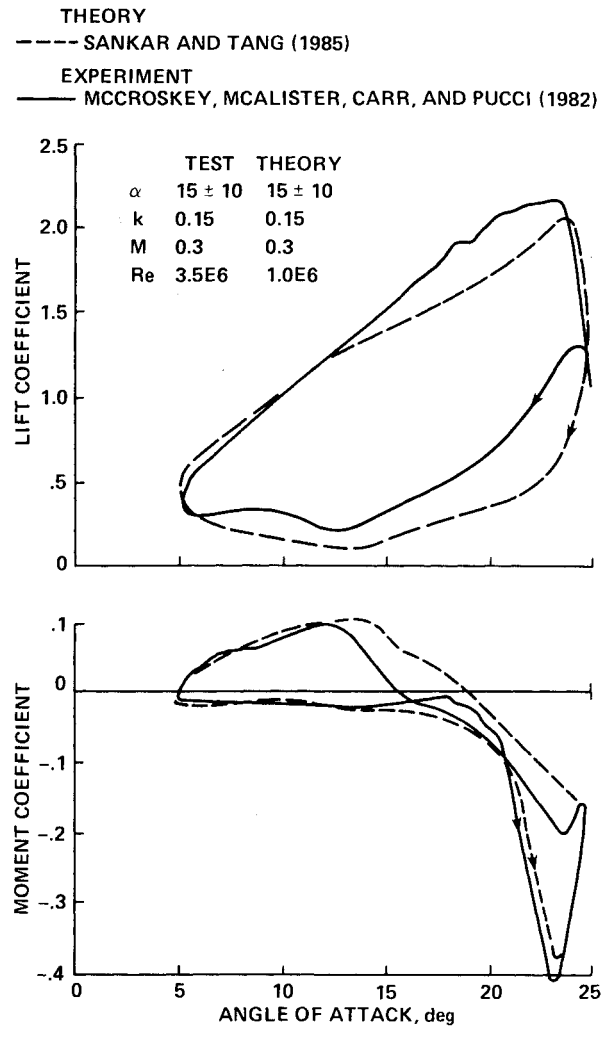

Fig. 20 Compressible, turbulent Navier-Stokes calculations of two-dimensional dynamic stall loads.[115]

Kocurek et al.[51,52,139] compared lifting surface theory, the L-method (as a one-chordwise panel version of the lifting surface method), and first-order lifting line theory for a hovering rotor blade. The one-panel lifting surface theory gave results as good as[51,52] or close to[139] those from the theory with five or seven chordwise panels, while the first-order lifting line theory gave significantly different results.

Formal lifting line theory is a solution for the three-dimensional wing loading obtained using the method of matched asymptotic expansions, based on the small parameter $\epsilon = c/R = 1/(\text{aspect ratio})$. The lowest-order three-dimensional effect for a nonrotating, steady, unswept wing in incompressible flow is Prandtl's theory. Higher-order theories have been developed by singular perturbation methods, beginning with the work of Van Dyke,[140] and lifting line theory has been extended to swept, unsteady, transonic, and rotating wings. The singular perturbation methods provide analytical solutions of the inner and outer problems, which are combined by the matching process.

Fixed-wing theories are applicable almost directly to the rotor problem, because the key to the method is the matching process and, in the matching domain, the rotor appears almost the same as the nonrotating wing. For the rotary wing, it is necessary to consider swept and yawed planforms, unsteady motion, and compressible or transonic flow. For the rotary wing, it is also necessary to include a high angle of attack (stall) in the inner solution and the helical, distorted, and rolled-up wake geometry in the outer solution. Hence, for the rotor, the theory must use numerical, rather than analytical, solutions of the inner and outer problems. It is not that simplifications are impossible. With undistorted geometry, the wake integrals can be evaluated analytically in the radial direction, although the helical nature requires a numerical integration over the wake age. Analytical solutions can be obtained for the linearized, inviscid inner problem, just as for fixed wings, although the solutions for higher-order lifting line theory are not simple. The value of lifting line theory in rotor problems, however, lies in the complexities that may be retained in the inner and outer problems. Analytical inner and outer solutions are not, in fact, needed, since the heart of the theory is the matching process. In the matching domain, the inner and outer problems can always be consistently simplified, without requiring that they be simple in their own domains. For the rotary wing, lifting line theory should provide the formulation of the inner and outer problems, and the matching that couples them, as the basis for an iterative numerical solution.

In the method of matched asymptotic expansions, the inner and outer solutions are expanded as series, with each term order ϵ smaller than its predecessor. Then, the n-term/m-order inner solution is matched to the m-term/n-order outer solution. At each level, the matching provides boundary conditions for the next term in the inner or outer expansion, from the solution at previous levels. For the high-aspect-ratio wing, the inner problem has simpler geometry (two-dimensional), but complex flow (Navier-Stokes equations). In the outer limit, the inner solution can be considered irrotational. The outer problem has complex geometry (the vortex wake), but irrotational flow. In the inner limit, the outer solution has simple geometry. In the matching domain, there is both simple geometry and irrotational flow.

Second-order lifting line theory was developed by Van Dyke.[140] Consider a nonrotating, unswept, steady wing in incompressible flow. Designate the order-n inner and outer solutions by ϕ_n^I and ϕ_n^O, respectively, since irrotational flow is assumed in the matching domain. The order-0 inner problem is a two-dimensional airfoil in a uniform freestream produced by the wing velocity. In the outer limit, the inner problem is irrotational and a solution of the two-dimensional Laplace's equation with regular boundary conditions at infinity can be expanded as a uniform flow, plus a bound vortex, plus a quadrupole, and so on. Then matching shows that the order-1 outer problem is a line of dipoles produced by the inner bound circulation Γ_0—a lifting line. In the inner limit, the outer problem appears to be an infinite bound vortex line and associated trailed vorticity, for which the solution can be expanded as a regular part (uniform velocity, linearly varying velocity, etc.) and a singular part (the bound circulation, a second-order term proportional to the second spanwise derivative of the bound circulation Γ_0'', etc.). The equation for a line of moving dipoles [Eq. (2)] can be used for the general case (rotating, swept, unsteady, and compressible); the Biot-Savart equation gives the solution for incompressible flow. Next, matching to ϕ_1^O shows that the order-1 inner problem is a two-dimensional airfoil, with zero boundary conditions at the airfoil surface and the wake-induced velocity v_i at infinity (a uniform freestream). Here, v_i is the lowest-order regular part of the outer solution at the lifting line—excluding the singular part, namely the bound vortex. This is Prandtl's first-order theory, as obtained by perturbation methods. Matching to ϕ_1^I, then shows that the order-2 outer problem is a dipole line produced by Γ_1 and a quadrupole line produced by Γ_0. Note that ϕ_2^O (with a quadrupole) is more singular in the inner limit than ϕ_1^O (a dipole line)—hence, the need for singular perturbation methods. Finally, the order-2 inner problem is an inhomogeneous equation, with a particular solution produced by the spanwise derivatives of ϕ_0^I. Matching gives the boundary conditions at infinity produced by ϕ_1^O and ϕ_2^O: a regular part (uniform and linearly varying induced velocity) and a singular part (proportional to Γ_0''). Again, ϕ_2^I is more singular in the outer limit than is ϕ_1^I. This is the second-order lifting line theory.

The order-2 outer solution has a quadrupole line produced by ϕ_0^I. The outer limit of ϕ_0^I is the same if the quadrupole strength is zero, but the bound vortex is offset. For a thin airfoil, the bound vortex must be at the quarter chord. Camber and thickness introduce additional chordwise and vertical shifts, respectively. The quadrupole strengths resulting from camber and thickness are not proportional to the bound circulation, so these shifts depend on the lift. They must be neglected, lest the outer problem geometry depend on the inner solution. With the bound vortex at the quarter chord then, only the dipole line is required in the outer solution—a wake of vortex sheets. The boundary condition for the order-2 inner problem involves a linearly varying induced velocity. For a thin airfoil, the correct lift is obtained with an induced velocity constant over the chord, if the value at the three-quarter chord is used. However, a linearly varying velocity would give a pitching moment, which the constant velocity does not. This version of the second-order theory may be compared with Weissinger's L-method,[136] in which the induced velocity is evaluated at the three-quarter chord, including the effect of the bound vortex at the quarter chord, and equated to the geometric angle of attack. The L-method is equivalent to using thin-airfoil theory for the inner solution (Pistolesi's theorem states that the velocity at one-half chord from the point bound vortex gives the correct boundary condition).

A remainder problem is defined by the order-2 inner problem, after accounting for the use of the induced velocity evaluated at the three-quarter chord. This problem has been solved by Van Dyke[140] for a constant angle of attack and by Van Holten[141-143] for a constant chord. In the practical implementation described above, the remainder problem is neglected; so the analytical solutions are useful as error estimates. Indeed, the lift error is small (second order) and so is the moment error, except probably the neglected moment from the linear variation of induced velocity.

As perturbation expansions, equivalent solutions are obtained if the inner problems are combined and all orders solved simultaneously. The combined inner problem is a two-dimensional airfoil in a uniform freestream, consisting of the wing motion and the wake-induced velocity. The induced velocity (three components) is evaluated at the three-quarter chord from the wake associated with a bound vortex line at the quarter chord (excluding the bound vortex, which has already been accounted for in the matching). Combining the ϕ_0^I and ϕ_1^I solutions is a natural step, since only an angle-of-attack change produced by the induced velocity is required. In the formal perturbation method, the solution alternates between the inner and outer problems: the two-dimensional airfoil with no wake is solved for Γ_0; the wake-induced velocity produced by Γ_0 is calculated; then the airfoil in the wake flowfield is solved for Γ_1. In the combined problem, however, the airfoil loading produced by the geometric angle of attack (ϕ_0^I) and by the wake-induced velocity (ϕ_1^I) are solved simultaneously and the induced velocity is evaluated from the total bound circulation ($\Gamma_0+\Gamma_1$), not from Γ_0 alone. Consequently, the direct solution of the perturbation method has been changed to an inverse solution (for example, the integral equation in Prandtl's theory). The inverse formulation is preferred, since it is found that the direct solution is too singular at the wing tips, where the theory is not strictly valid.[140] The inverse solution (from an integral equation) is well behaved, even for rectangular tip wings.

Swept-wing, incompressible lifting line theory has been developed by Cheng for straight planforms[144] and for curved planforms.[145] If the wing curvature is order ϵ^2 small, the differential equations for ϕ_0^I and ϕ_1^I remain two-dimensional; if the curvature is order ϵ, the ϕ_1^I equation has an inhomogeneous term. Small curvature is typical of rotor blades, except at kinks in the planform. At kinks, the asymptotic expansion used is invalid to any order; the integral equation formulation must be relied on to keep the solution well behaved. For swept wings, the inner limit of the dipole and quadrupole lines has singular terms proportional to $\Gamma'\tan\Lambda$ (where Λ is the local sweep angle). Then, by matching, the inner problem boundary condition at infinity consists of not only the induced velocity (regular part of the swept wake solution), but also these singular terms produced by sweep. It can be shown that, if the induced velocity is calculated at the three-quarter chord and these new swept-wing boundary conditions are ignored, the wing lift is correct but that there will be a moment error. Experience with the L-method confirms that this is a good approximation to the second-order lifting line theory for the wing lift distribution.

Unsteady lifting line theory has been developed by Van Holten[146] and Ahmadi[147] for $k \triangleq \epsilon$ and by Cheng[145] and Guiraud and Slama[148] for $k \triangleq 1$. The order-0 inner problem is an unsteady two-dimensional airfoil in a swept freestream produced by the wing motion with a two-dimensional shed wake. The order-1 outer problem is again a lifting line, matching both the bound vorticity and the shed wake of ϕ_0^I. The boundary condition at infinity for the order-1 inner problem again consists of the induced velocity (regular part) and a singular part produced by sweep, from which must be excluded now not only the bound vortex but also the inner shed wake,[146,147] since both have already been accounted for in matching ϕ_0^I to ϕ_1^O. The unsteady wake-induced velocity is a function of $(t-x/U)$, like a convected gust.[146,147] The variation of the induced velocity over the chord is then order k and, assuming the velocity is constant over the chord, is consistent for $k \triangleq \epsilon$. For $k \triangleq 1$, the induced velocities (three-

dimensional effects) are really order ϵ smaller than for steady loading.[145,148]

It is also possible in unsteady lifting line theory to consider the shed wake not in the inner problem itself, but as part of the boundary conditions for the inner problem. Then, only the bound vortex would be excluded from the induced velocity. The entire shed wake would be part of the outer problem and the shed wake would be excluded from the inner problem. For complex wing motion and wake geometry (such as with a rotor blade), it is probably easier to ensure consistency between the outer and inner wake models with this approach. However, one difficulty is that the inner shed wake begins at the trailing edge, while the outer wake emanates from the bound vortex line. It is also natural to attempt to treat the shed wake and trailed wake identically: to evaluate the induced velocity at the three-quarter chord and use it as a uniform freestream in the inner problem. Piziali[149] developed a way to combine the outer wake and inner shed wake by evaluating the induced velocity along the blade chord from all sources and applying thin airfoil theory. Miller[150] used the induced velocity at the three-quarter chord and modified the shed wake model as required to obtain the correct unsteady loads. Considering unsteady airfoil motion,[1,13,150] the Theodorsen function is matched well (at least to first order in k and in practice for $k \triangleq 1$) with the induced velocity evaluated at the three-quarter chord and the shed wake started at the trailing edge. Considering a convected gust, the Sears function is also well matched, although there is a moment error. Hence, assuming that the shed and trailed wake-induced velocity is constant over the chord is a good approximation for $k \triangleq \epsilon$; while for $k \triangleq 1$ the three-dimensional unsteady effects are of higher order and the two-dimensional unsteady effects (the Theodorsen function) are still well approximated. It is consistent to have the unsteady inner solution accurate to $k \triangleq 1$ (for which the three-dimensional effects are of second order) and the unsteady outer solution accurate to $k \triangleq \epsilon$ (for which the three-dimensional effects are of first order, but the induced velocity can be considered constant over the chord).

Compressible lifting line theory for an unswept, steady wing can be scaled to the incompressible problem by the Prandtl-Glauert transformations. For a swept wing, the order-1 inner equation has an inhomogeneous term proportional to $M_x M_y$, unless this product is order ϵ. For a rotor blade, the maximum value of $M_x M_y \cong M_{\text{tip}}^2 \mu$, which is typically around 0.25; so the inhomogeneous term should have a relatively small effect. Recall that ϕ_1^1 must match at infinity the singular term (proportional to $\Gamma' \tan\Lambda$), from the dipole-line outer solution (now compressible). The particular solution has no lift (although a nonzero moment) and its outer limit combines with the boundary condition from the outer solution such that the total scales to the incompressible problem. Hence, neglecting these effects for a compressible flow, which is necessary if the order-1 inner problem is to remain two-dimensional, adds no more error than for incompressible flow. For unsteady motion with $k \triangleq 1$, the time derivatives in the equation of motion must be retained at the lowest order: the problem for ϕ_0^1 is unsteady and compressible. For $k \triangleq \epsilon$, the ϕ_0^1 equation is quasistatic—the unsteady effects enter only through the wake and boundary conditions. The wake solution for a steady nonrotating wing, as well as for unsteady motion at low frequency, can be scaled to the incompressible solution. However, lifting line theory as implemented in rotary-wing analysis almost never uses a compressible wake; the outer problem is assumed to be incompressible.

Transonic lifting line theory has been developed by Cook and Cole[151] for an unswept wing and by Cook[152] and Cheng et al.[153-155] for a swept wing. The flow is first expanded in powers of $\tau^{2/3}$, with the usual transonic scaling, to obtain the small-disturbance equation. Then, the solution is expanded in the lifting line parameter ϵ. In order to be consistent with the transonic scaling,[151,153] $\epsilon = \tau^{-1/3} c/R$. So to achieve a given accuracy of the lifting line theory, a larger aspect ratio is required in the transonic flow. It is also not consistent to construct transonic lifting line theory beyond first order without also considering the next term in the transonic expansion. For an unswept, steady wing, the order-0 inner problem is the transonic two-dimensional equation, the order-1 outer problem is the subsonic (linear) equation, and the order-1 inner problem is the transonic equation linearized about ϕ_0^1. Nonlinearity does not enter the matching to first order: ϕ_1^0 is a lifting line and the wake-induced velocity gives the boundary condition for ϕ_1^1. Nonlinearity appears in the matching to establish the form of ϕ_2^0.[151] The outer limit of ϕ_0^1 has now a term produced by the nonlinearity of the transonic equation. A particular solution of ϕ_1^0 is required by the inhomogeneous term in the equation (which is the transonic equation linearized about ϕ_1^0). These two manifestations of the same nonlinearity cancel exactly in the matching; the solution of the homogeneous equation for ϕ_2^0 remains a dipole and quadrupole line. If the inner problems for ϕ_0^1 and ϕ_1^1 are not recombined, it is also necessary to consider perturbation of the shock jump relations and the shock position.[151,153,154] For a swept wing, the transonic scaling requires $M_y \triangleq \tau^{1/3}$ or smaller. Then, unless $M_x M_y \triangleq \tau^{1/3} \epsilon = c/R$, there will still be the inhomogeneous term proportional to $M_x M_y$ in the ϕ_1^1 equation,[152,153] with a particular solution as for subsonic flow. Recall that ϕ_1^1 has a boundary condition at infinity proportional to $\Gamma' \tan\Lambda$ as a result of matching to the outer solution. In the subsonic case, the particular solution has an outer limit of the same form and same order as the boundary condition. In the transonic case, it happens that the outer limit of the particular solution exactly matches the boundary condition to the lowest order. For unsteady flow, transonic scaling requires $k \triangleq \tau^{2/3}$. Then, the order-0 inner equation is transonic and unsteady, regardless of ϵ.

In viscous lifting line theory, by assuming that the outer limit of the inner problem is still irrotational, it follows that the matching results are the same as for inviscid flow. As usual, it is desired that the inner problem be two-dimensional to at least first order (more generally, an infinite-aspect-ratio, yawed wing). For the spanwise derivatives in the viscous equations to be of second order or smaller requires only that the Reynolds number based on the chord be order 1 ($Re \triangleq 1$, viscous domain of the order of the chord) for upswept wings or $Re \triangleq \epsilon^{-1}$ for swept wings. In fact, the Reynolds number is five or six orders larger than ϵ^{-1} for helicopter rotors. Hence, the lifting line assumption is easily satisfied regarding viscous transport, since the equations imply that the viscous effects are confined to thin layers. What must really be considered is the geometry of the flowfield, such as large-scale separation, that results from the introduction of viscosity; that geometry must vary slowly in the spanwise direction.

Rotary-wing lifting line theory must be developed in a rotating and translating coordinate system, where the wing velocities vary along the span and with time. The geometry of the wing (possibly swept) relative to the moving frame can be described just as for a fixed wing. Basically, the inner problem remains two-dimensional and the inner limit of the outer problem looks like a nonrotating wing. Therefore, rotation of the wing introduces some complications, but no major assumptions beyond those needed for the fixed wing. For the incompressible case, the flow is still described by Laplace's equation in the matching domain (irrotational flow); thus, rotation of the wing enters only through the boundary conditions and the wake geometry. For the compressible case, additional Coriolis and centrifugal-type terms appear in the equations of motion. The consequence is just another inhomogeneous term proportional to M_y in the ϕ_1^1 equation. In the inner limit of the wake solution, it is appropriate to neglect the vertical component and the spanwise variation of the magnitude and sweep angle of the freestream

velocity and to assume a small retarded time for the compressible flow. The result is identical to the inner limit for a fixed wing. Van Holten[141-143] developed a second-order lifting line theory for a rotary wing using the method of matched asymptotic expansions. The effects of sweep and unsteady motion were considered for inviscid and incompressible flow. An analytical inner solution was obtained for a thin wing; the acceleration potential was used, implying an undistorted wake geometry. Vaidyanathan and Pierce[156,157] applied Van Holten's theory to the calculation of rotor air loads. For a better wake geometry, the mean induced velocity was included in the nonrotating frame air velocity. A discretized version of the theory was developed in place of numerical integration over the wake age to reduce the computation times.

Conclusions

The progress in development of advanced computational methods for rotary-wing aerodynamics has been reviewed. It is a measure of the speed at which progress is being made that numerous papers have been published in the field since this review was prepared, with a number of notable achievements and several interesting comparisons of methods for particular problems.[158,159]

Key aspects of helicopter aerodynamics are the importance of the wake influence in almost all problems and of the viscous effects, particularly in stall and wake formation, for even moderate operating conditions. Lifting line theory will remain the foundation for general rotary-wing aerodynamics calculations as long as it is the only practical viscous method for rotors. Lifting line theory is both more widely applicable and more complex than is generally acknowledged. Despite its usefulness and success, it requires numerous approximations and assumptions. Developing an improved or higher-order lifting line theory would likely require further approximations in order to maintain the practicality of the method. So further advances will come by developing methods to replace the lifting line theory.

In the lifting surface theory, the use of the acceleration potential precludes incorporating a distorted wake in any simple manner and the kernel is fundamentally more complicated than for fixed wings. Hence, the theory will never be the basis for a general-purpose analysis of helicopter rotors, but it does provide a sound starting point for simplified models, such as a compressible dynamic-inflow theory.

In panel methods for helicopter fuselages, it is still not possible to accurately model separation. The influence of a rotor on the body has been considered using only actuator disk models of the rotor, yet it is known that the unsteady body loads are significant. Rotor calculations have been applied to hover only, again in the steady case. A true compressible method is needed for rotors and panel methods should be applied to unsteady problems. More work will be required on free-wake geometry models as a part of the panel methods.

In transonic flow problems on rotors, the Euler equations are beginning to be solved for phenomena that are inviscid but not irrotational and isentropic. The Euler equations may enable calculations of the tip vortex formation, but there are unquestionably viscous effects that will require solutions of the Navier-Stokes equations. For some time, it will remain necessary to restrict the extent of the computation domain in such methods; so it will continue to be necessary to develop techniques to couple the finite difference methods with global models of the rotor wake and blade motion.

Continued work on predicting dynamic stall must include methods for cases dominated by the leading-edge vortex. Turbulence modeling naturally constitutes a major limitation on the calculation of helicopter flowfields. Current investigations do not indicate any universally accepted approach for wake modeling. A rigorous and direct attack on the problem of wake formation and development is needed, for it is the wake that most distinguishes the rotary-wing problems from their fixed wing counterparts.

The goal of turbulent Navier-Stokes calculations for an entire rotorcraft is not in sight, but the capabilities of current algorithms and machines at least make it possible to begin work on the problem, with good prospects for progress. Advances in helicopter aerodynamic computations will continue to be made by considering idealized and model problems and by the use of hybrid methods to produce efficient and practical tools.

References

[1]Johnson, W., *Helicopter Theory*, Princeton University Press, Princeton, NJ, 1980.

[2]Ashley, H. and Landahl, M., *Aerodynamics of Wings and Bodies*, Addison-Wesley Publishing Co., Reading, MA, 1965.

[3]Garrick, I. E., "Nonsteady Wing Characteristics," *Aerodynamic Components of Aircraft at High Speeds*, edited by A. E. Donovan and H. R. Lawrence, Princeton University Press, Princeton, NJ, 1957.

[4]Farassat, F., "Theory of Noise Generation from Moving Bodies with an Application to Helicopter Rotors," NASA TR R-451, Dec. 1975.

[5]Dat, R., "Lifting Surface Theory Applied to Fixed Wings and Propellers," European Space Research Organization, Paris, Rept. ESRO TT-90, Sept. 1974.

[6]Farassat, F., "Advanced Theoretical Treatment of Propeller Noise," von Kármán Institute, Brussels, Lecture Series 81-82/10, May 1982.

[7]Dat, R., "Representation of a Lifting Line in an Arbitrary Motion by a Line of Acceleration Doublets," NASA TT F-12952, May 1970.

[8]Dat, R., "Aeroelasticity of Rotary Wing Aircraft," AGARD Lecture Series 63, 1973.

[9]Costes, J. J., "Computation of Unsteady Aerodynamic Forces on Helicopter Rotor Blades," AGARD Rept. 595, April 1972 (also NASA TT F-15039).

[10]Watkins, C. E., Runyan, H. L., and Woolston, D. S., "On the Kernel Function of the Integral Equation Relating the Lift and Downwash Distribution of Oscillating Finite Wings in Subsonic Flow," NACA Rept. 1234, 1955.

[11]Landahl, M. T., "Kernel Function for Nonplanar Oscillating Surfaces in a Subsonic Flow," *AIAA Journal*, Vol. 5, May 1967.

[12]Sopher, R., "Three-Dimensional Potential Flow Past the Surface of a Rotor Blade," Paper presented at Annual National Forum of American Helicopter Society, May 1969.

[13]Costes, J. J., "Application of the Lifting Line Concept to Helicopter Computation," Paper presented at European Rotorcraft and Powered Lift Aircraft Forum, Sept. 1978.

[14]Hanson, D. B., "Compressible Helicoidal Surface Theory for Propeller Aerodynamics and Noise," *AIAA Journal*, Vol. 21, June 1983.

[15]Hanson, D. B., "Compressible Lifting Surface Theory for Propeller Performance Calculation," *Journal of Aircraft*, Vol. 22, Jan. 1985.

[16]Runyan, H. L. and Tai, H., "Lifting Surface Theory for a Helicopter Rotor in Forward Flight," NASA CR 169997, 1983.

[17]Tai, H. and Runyan, H. L., "Lifting Surface Theory for a Helicopter Rotor in Forward Flight," Paper presented at American Helicopter Society Specialists' Meeting on Rotorcraft Dynamics, Nov. 1984.

[18]Lamb, H., *Hydrodynamics*, Dover Publications, New York, 1932.

[19]Margason, R. J. et al., "Subsonic Panel Methods—A Comparison of Several Production Codes," AIAA Paper 85-0280, Jan. 1985.

[20]Maskew, B., "Prediction of Subsonic Aerodynamic Characteristics: A Case for Low-Order Panel Methods," *Journal of Aircraft*, Vol. 19, Feb. 1982.

[21]Clark, D. R. and Maskew, B., "Study for Prediction of Rotor/Wake/Fuselage Interference," NASA CR 177340, March 1985.

[22]Morino, L., "A General Theory of Unsteady Compressible Potential Aerodynamics," NASA CR 2464, Dec. 1974.

[23]Mangler, K. W. and Smith, J. H. B., "Behavior of the Vortex Sheet at the Trailing Edge of a Lifting Wing," *Aeronautical Journal*, Vol. 74, Nov. 1970.

[24]Hess, J. L., "The Problem of Three-Dimensional Lifting Potential Flow and Its Solution by Means of Surface Singularity Distribution," *Computer Methods in Applied Mechanics and Engineering*, Vol. 4, No. 3, Nov. 1974.

[25]Morino, L., Kaprielian, A. Jr., and Sipcic, S. B., "Free Wake Aerodynamic Analysis of Helicopter Rotors," Boston University, Boston, Rept. CCAD TR 83-01, May 1983.

[26]Summa, J. M., "Potential Flow About Three Dimensional Lifting Configurations with Application to Wings and Rotors," AIAA Paper 75-126, Jan. 1975.

[27]Morse, P. M. and Feshbach, H., *Methods of Theoretical Physics*, McGraw-Hill Book Co., New York, 1953.

[28]Hess, J. L. and Smith, A. M. O., "Calculation of Potential Flow about Arbitrary Bodies," *Progress in Aeronautical Sciences*, Vol. 8, edited by D. Kuchemann, Pergamon Press, Oxford, England, 1966.

[29]Rubbert, P. E. and Saaris, G. R., "3-D Potential Flow Method Predicts V/STOL Aerodynamics," *SAE Journal*, Vol. 77, Sept. 1969.

[30]Rubbert, P. E. and Saaris, G. R., "Review and Evaluation of a Three-Dimensional Lifting Potential Flow Analysis Method for Arbitrary Configurations," AIAA Paper 72-188, Jan. 1972.

[31]Djojodihardjo, R. H. and Widnall, S. E., "A Numerical Method for the Calculation of Nonlinear, Unsteady Lifting Potential Flow Problems," *AIAA Journal*, Vol. 7, Oct. 1969.

[32]Morino, L. and Kuo, C.-C., "Subsonic Potential Aerodynamics for Complex Configurations: A General Theory," *AIAA Journal*, Vol. 12, Feb. 1974.

[33]Maskew, B., "Program VSAERO—A Computer Program for Calculating the Nonlinear Aerodynamic Characteristics of Arbitrary Configurations," NASA CR 166476, Dec. 1982.

[34]Gillespie, J. Jr., "An Investigation of the Flow Field and Drag of Helicopter Fuselage Configurations," Paper presented at Annual National Forum of American Helicopter Society, May 1973.

[35]Gillespie, J. Jr. and Windsor, R. I., "An Experimental and Analytical Investigation of the Potential Flow Field, Boundary Layer, and Drag of Various Helicopter Fuselage Configurations," U.S. Army Air Mobility Research and Development Laboratories, TN 13, Jan. 1974.

[36]Gillespie, J. Jr., "Streamline Calculations Using the XYZ Potential Flow Program," U.S. Army Air Mobility Research and Development Laboratories, TN 16, May 1974.

[37]Woodward, F. A., Dvorak, F. A., and Geller, E. W., "A Computer Program for Three Dimensional Lifting Bodies in Subsonic Inviscid Flow," U.S. Army Air Mobility Research and Development Laboratories, TR 74-18, April 1974.

[38]Dvorak, F. A., Maskew, B., and Woodward, F. A., "Investigation of Three-Dimensional Flow Separation and Fuselage Configurations," U.S. Army Air Mobility Research and Development Laboratories, TR 77-4, March 1977.

[39]Clark, D. R., Dvorak, F. A., Maskew, B., Summa, J. M., and Woodward, F. A., "Helicopter Flow Field Analysis," U.S. Army Research and Technology Laboratories, TR 79-4, April 1979.

[40]Sheehy, T. W., "A Simplified Approach to Generalized Helicopter Configuration Modeling and the Prediction of Fuselage Surface Pressures," *Journal of the American Helicopter Society*, Vol. 21, No. 1, Jan. 1976.

[41]Soohoo, P., Noll, R. B., Morino, L., and Ham, N. D., "Rotor Wake Effects on Hub/Pylon Flow," U.S. Army Research and Technology Laboratories, TR 78-1, May 1978.

[42]Polz, G. and Quentin, J., "Separated Flow Around Helicopter Bodies," Paper presented at European Rotorcraft and Powered Lift Aircraft Forum, Sept. 1981.

[43]Maskew, B., "Influence of Rotor Blade Tip Shape on Tip Vortex Shedding—An Unsteady, Inviscid Analysis," Paper presented at Annual National Forum of American Helicopter Society, May 1980.

[44]Maskew, B. and Rao, B. M., "Unsteady Analysis of Rotor Blade Tip Flow," NASA CR 3868, May 1985.

[45]Maskew, B. and Dvorak, F. A., "The Prediction of Climax Using a Separated Flow Model," *Journal of the American Helicopter Society*, Vol. 23, No. 2, April 1978.

[46]Costes, J. J., "Theoretical Study of Two Dimensional Stall in an Incompressible Flow," Paper presented at European Rotorcraft Forum, Aug. 1984.

[47]Freeman, C. E., "Development and Validation of a Combined Rotor-Fuselage Induced Flow-Field Computational Method," NASA TP 1656, June 1980.

[48]Clark, D. R. and Maskew, B., "Calculation of Rotor/Airframe Interference for Realistic Configurations," Paper presented at European Rotorcraft and Powered Lift Aircraft Forum, Sept. 1982.

[49]Clark, D. R., "Analysis of the Wing/Rotor and Rotor/Rotor Interactions Present in Tilt-Rotor Aircraft," Paper presented at AHS/ARO International Conference on Rotorcraft Basic Research, Feb. 1985.

[50]Csencsitz, T. A., Fanucci, J. B., and Chou, H. F., "Nonlinear Helicopter Rotor Lifting Surface Theory," West Virginia University, Morgantown, Aerospace Engineering Rept. TR-35, Sept. 1973.

[51]Kocurek, J. D. and Tangler, J. L., "A Prescribed Wake Lifting Surface Hover Performance Analysis," *Journal of the American Helicopter Society*, Vol. 22, No. 1, Jan. 1977.

[52]Kocurek, J. D., "A Lifting Surface Performance Analysis with Circulation Coupled Wake for Advanced Configuration Hovering Rotors," Ph.D. Thesis, Texas A&M University, College Station, May 1978.

[53]Summa, J. M. and Clark, D. R., "A Lifting-Surface Method for Hover/Climb Airloads," Paper presented at Annual National Forum of American Helicopter Society, May 1979.

[54]Summa, J. M., "Advanced Rotor Analysis Methods for the Aerodynamics of Vortex/Blade Interactions in Hover," Paper presented at European Rotorcraft and Powered Lift Aircraft Forum, Sept. 1982.

[55]Summa, J. M. and Maskew, B., "A Surface Singularity Method for Rotors in Hover or Climb," U.S. Army Aviation Research and Development Command, TR 81-D-23, Dec. 1981.

[56]Shenoy, K. R. and Gray, R. B., "Iterative Lifting Surface Method for Thick Bladed Hovering Helicopter Rotors," *Journal of Aircraft*, Vol. 18, June 1981.

[57]Morino, L. and Soohoo, P., "Green's Function Method for Compressible Unsteady Potential Aerodynamic Analysis of Rotor-Fuselage Interaction," Paper presented at European Rotorcraft and Powered Lift Aircraft Forum, Sept. 1978.

[58]Preuss, R. D., Suciu, E. O., and Morino, L., "Unsteady Potential Aerodynamics of Rotors with Applications to Horizontal Axis Windmills," *AIAA Journal*, Vol. 18, April 1980.

[59]Morino, L., Kaprielian, Z. Jr., and Sipcic, S. R., "Free Wake Analysis of Helicopter Rotors," *Vertica*, Vol. 9, No. 2, 1985.

[60]McMahon, H. M., Komerath, N. M., and Hubbartt, J. E., "Studies of Rotor-Airframe Interaction in Forward Flight," AIAA Paper 85-5015, Oct. 1985.

[61]Kawachi, K., "Extension of Local Momentum Theory to Hovering Rotor with Distorted Wake," *Journal of Aircraft*, Vol. 19, July 1982.

[62]Wirz, H. J. and Smolderen, J. J. (eds.), *Numerical Methods in Fluid Dynamics*, Hemisphere Publishing Corp., Washington, DC, 1978.

[63]Isom, M. P., "Unsteady Subsonic and Transonic Potential Flow over Helicopter Rotor Blades," NASA CR 2463, Oct. 1974.

[64]Caradonna, F. X. and Isom, M. P., "Numerical Calculation of Unsteady Transonic Potential Flow over Helicopter Rotor Blades," *AIAA Journal*, Vol. 14, April 1976.

[65]Murman, E. M. and Cole, J. D., "Calculation of Plane Steady Transonic Flows," *AIAA Journal*, Vol. 9, Jan. 1971.

[66]Caradonna, F. X. and Isom, M. P., "Subsonic and Transonic Potential Flow over Helicopter Rotor Blades," *AIAA Journal*, Vol. 10, Dec. 1972.

[67]Ballhaus, W. F. and Caradonna, F. X., "The Effect of Planform Shape on the Transonic Flow Past Rotor Tips," AGARD CP 111, Sept. 1972.

[68]Caradonna, F. X., "The Transonic Flow on a Helicopter Rotor," Stanford University, Stanford, CA, Ph.D. Thesis, March 1978.

[69]Caradonna, F. X. and Philippe, J. J., "The Flow over a Helicopter Blade Tip in the Transonic Regime," *Vertica*, Vol. 2, No. 1, 1978.

[70]Caradonna, F. X., "Finite Difference Methods for the Solution of Unsteady Potential Flows," NASA TM 84248, June 1982.

[71]Chattot, J. J., "Calculation of Three-Dimensional Unsteady Transonic Flows Past Helicopter Blades," NASA TP 1721, Oct. 1980.

[72]Chattot, J. J. and Philippe, J. J., "Pressure Distribution Computation on a Non-Lifting Symmetrical Helicopter Blade in Forward Flight," La Recherche Aerospatiale, No. 1980-5, 1980.

[73]Philippe, J. J. and Chattot, J. J., "Experimental and Theoretical Studies on Helicopter Blade Tips at ONERA," Paper presented at European Rotorcraft and Powered Lift Aircraft Forum, Sept. 1980.

[74]Caradonna, F. X., Desopper, A., and Tung, C., "Finite Difference Modeling of Rotor Flows Including Wake Effects," *Journal of the American Helicopter Society*, Vol. 29, No. 2, April 1984.

[75]Tung, C., Caradonna, F. X., Boxwell, D. A., and Johnson, W., "The Prediction of Transonic Flows on Advancing Rotors," Paper presented at Annual National Forum of American Helicopter Society, May 1984.

[76]Desopper, A., "Study of the Unsteady Transonic Flow on Rotor Blade with Different Tip Shapes," Paper presented at European Rotorcraft Forum, Aug. 1984.

[77]Grant, J., "Calculation of Supercritical Flow Over the Tip Region of a Rotor Blade at Arbitrary Azimuth," *Numerical Methods in Applied Fluid Dynamics*, edited by B. Hunt, Academic Press, London, 1980.

[78]Grant, J., "The Prediction of Supercritical Pressure Distributions on Blade Tips of Arbitrary Shape Over a Range of Advancing Blade Azimuth Angles," *Vertica*, Vol. 2, Nos. 3-4, 1979.

[79]Riley, M J. and Miller, J. V., "Pressure Distributions on a Helicopter Swept Tip from Flight Tests and from Calculations," Paper presented at European Rotorcraft Forum, Sept. 1983.

[80]Stahl, H., "Calculation of 3D Unsteady Transonic Flow Around Rotor Blades," AGARD CP 334, May 1982.

[81]Stahl, H., "The Problem of Calculation of the Flow Around Helicopter Rotor Blade Tips," Paper presented at European Rotorcraft and Powered Lift Aircraft Forum, Sept. 1981.

[82]Arieli, R. and Tauber, M. E., "Analysis of the Quasi-Steady Flow about an Isolated Lifting Helicopter Rotor Blade," Joint Institute for Aeronautics and Acoustics, Stanford University, Stanford, CA, JIAA TR-24, Aug. 1979.

[83]Arieli, R. and Tauber, M. E., "Computation of Subsonic and Transonic Flow about Lifting Rotor Blades," AIAA Paper 79-1667, Aug. 1979.

[84]Tauber, M. E., Chang, I.-C., Caughey, D. A., and Philippe, J. J., "Comparison of Calculated and Measured Pressures on Straight- and Swept-Tip Model Rotor Blades," NASA TM 85872, Dec. 1983.

[85]Dulikravich, D. S., "WIND—Computer Program for Calculation of Three-Dimensional Potential Compressible Flow about Wind Turbine Rotor Blades," NASA TP 1729, Oct. 1980.

[86]Chang, I-C., "Transonic Flow Analysis for Rotors," NASA TP 2375, July 1984.

[87]Chang, I-C. and Tung, C., "Numerical Solution of the Full-Potential Equation for Rotors and Oblique Wings Using a New Wake Model," AIAA Paper 85-0268, Jan. 1985.

[88]Tung, C. and Chang, I-C., "Rotor Transonic Computation with Wake Effects," Paper presented at Fourth International Conference on Applied Numerical Modeling, Dec. 1984.

[89]Sanker, L. N. and Prichard, D., "Solution of Transonic Flow Past Rotor Blades Using the Conservative Full Potential Equation," AIAA Paper 85-5012, Oct. 1985.

[90]Wake, B. E., Sankar, N. L., and Lekoudis, S. G., "Computation of Rotor Blade Flows Using Euler Equations," AIAA Paper 5010, Oct. 1985.

[91]Johnson, W., "Development of a Comprehensive Analysis for Rotorcraft," *Vertica*, Vol. 5, Nos. 2-3, 1981.

[92]Boxwell, D. A., Schmitz, F. H., Splettstoesser, W. R., and Schultz, K. J., "Model Helicopter Rotor High-Speed Impulsive Noise: Measured Acoustics and Blade Pressures," Paper presented at European Rotorcraft Forum, Sept. 1983.

[93]Scully, M. P., "Computation of Helicopter Rotor Wake Geometry and Its Influence on Rotor Harmonic Airloads," Massachusetts Institute of Technology, Cambridge, ASRL TR 178-1, March 1975.

[94]Clark, D. R. and Landgrebe, A. J., "Wake and Boundary Layer Effects in Helicopter Rotor Aerodynamics," AIAA Paper 71-581, June 1971.

[95]Clark, D. R. and Leiper, A. C., "The Free Wake Analysis, A Method for the Prediction of Helicopter Rotor Hovering Performance," *Journal of the American Helicopter Society*, Vol. 15, No. 1, Jan. 1970.

[96]Miller, R. H., "A Simplified Approach to the Free Wake Analysis of a Hovering Rotor," *Vertica*, Vol. 6, No. 2, 1982.

[97]Murman, E. M. and Stremel, P. M., "A Vortex Wake Capturing Method for Potential Flow Calculations," AIAA Paper 82-0947, June 1982.

[98]Stremel, P. M., "Computational Methods for Non-Linear Vortex Wake Flow Fields with Applications to Conventional and Rotating Wings," M.S. Thesis, Massachusetts Institute of Technology, Cambridge, Feb. 1982.

[99]Stremel, P. M., "A Method for Modeling Finite Core Vortices in Wake Flow Calculations," AIAA Paper 84-0417, Jan. 1984.

[100]Roberts, T. W., "Computation of Potential Flows with Embedded Vortex Rings and Applications of Helicopter Rotor Wakes," Massachusetts Institute of Technology, Cambridge, CFDL-TR 83-5, Sept. 1983.

[101]Roberts, T. W. and Murman, E. M., "A Computational Method for Helicopter Vortex Wakes," AIAA Paper 84-1554, June 1984.

[102]Liu, C H., Thomas, J. L., and Tung, C., "Navier-Stokes Calculations for the Vortex Wake of a Rotor in Hover," AIAA Paper 83-1676, July 1983.

[103]Cantaloube, B. and Huberson, S., "A New Approach Using Vortex Point Method for Prediction of Rotor Performance in Hover and Forward Flight," Paper presented at European Rotorcraft Forum, Sept. 1983.

[104]Cantaloube, B., "Numerical Calculation of Rotor Performance in Real Flight Configurations," Paper presented at AHS/ARO International Conference on Rotorcraft Basic Research, Feb. 1985.

[105]Egolf, T. A. and Sparks, S. P., "Hovering Rotor Airload Prediction Using a Full Potential Flow Analysis with Realistic Wake Geometry," Paper presented at Annual National Forum of American Helicopter Society, May 1985.

[106]Roberts, T. W. and Murman, E. M., "Solution Method for a Hovering Helicopter Rotor Using the Euler Equations," AIAA Paper 85-0436, Jan. 1985.

[107]Sankar, N. L., Wake, B. E., and Lekoudis, S. G., "Solution of the Unsteady Euler Equations for Fixed and Rotor Wing Configurations," AIAA Paper 85-0120, Jan. 1985.

[108]Srinivasan, G. R., Chyu, W. J., and Steger, J. L., "Computation of Simple Three-Dimensional Wing-Vortex Interaction in Transonic Flow," AIAA Paper 81-1206, June 1981.

[109]George, A. R. and Chang, S. B., "Noise Due to Transonic Blade-Vortex Interactions," Paper presented at Annual National Forum of American Helicopter Society, May 1983.

[110]George, A. R. and Chang, S. B., "Flow Field and Acoustics of Two-Dimensional Transonic Blade-Vortex Interaction," AIAA Paper 84-2309, Oct. 1984.

[111]McCroskey, W. J. and Goorjian, P. M., "Interactions of Airfoils with Gusts and Concentrated Vortices in Unsteady Transonic Flow," AIAA Paper 83-1691, July 1983.

[112]Srinivasan, G. R., McCroskey, W. J., and Kutler, P., "Numerical Simulation of the Interaction of a Vortex with Stationary Airfoil in Transonic Flow," AIAA Paper 84-0254, Jan. 1984.

[113]McCroskey, W. J. and Srinivasan, G. R., "Transonic Interaction of Unsteady Vortical Flows," NASA TM 86658, Dec. 1984.

[114]Srinivasan, G. R., McCroskey, W. J., and Baeder, J. D., "Aerodynamics of Two-Dimensional Blade-Vortex Interactions," AIAA Paper 85-1560, July 1985.

[115]Sankar, N. L. and Tang, W., "Numerical Solution of Unsteady Viscous Flow Past Rotor Sections," AIAA Paper 85-0129, Jan. 1985.

[116]Wu, J. C., Sankar, N. L., and Hsu, T. M., "Unsteady Aerodynamics of Airfoil Encountering a Passing Vortex," AIAA Paper 85-0203, Jan. 1985.

[117]Ballhaus, W. F. and Goorjian, P. M., "Implicit Finite-Difference Computations of Unsteady Transonic Flows about Airfoils," *AIAA Journal*, Vol. 15, Dec. 1977.

[118]McCroskey, W. J., Kutler, P., and Bridgeman, J. O., "Status and Prospects of Computational Fluid Dynamics for Unsteady Transonic Viscous Flows," AGARD CP 374, Sept. 1984.

[119]McCroskey, W. J. and Baeder, J. D., "Some Recent Advances in Computational Aerodynamics for Helicopter Applications," NASA TM 86777, Oct. 1985.

[120]McCroskey, W. J., "The Phenomenon of Dynamic Stall," NASA TM 81264, March 1981.

[121]McCroskey, W. J. and Pucci, S. L., "Viscous-Inviscid Interaction on Oscillating Airfoils in Subsonic Flow," *AIAA Journal*, Vol. 20, Feb. 1982.

[122]McCroskey, W. J., "Recent Developments in Dynamic Stall," *Proceedings of Symposium on Unsteady Aerodynamics*, edited by R. B. Kinney, Tucson, AZ, March 1975.

[123]Ham, N. D., "Aerodynamic Loading on a Two-Dimensional Airfoil During Dynamic Stall," *AIAA Journal*, Vol. 6, Oct. 1968.

[124]Baudu, N., Sagner, M., and Souquet, J., "Modelisation du Dechrochage Dynamique d'un Profil Oscillant," Paper presented at AAAF 10th Colloque d'Aeronautique Appliquee, 1973.

[125]Ono, K., Kuwahara, K., and Oshima, K., "Numerical Analysis of Dynamic Stall Phenomena of an Oscillating Airfoil by the Discrete Vortex Approximation," Paper presented at Seventh International Conference on Numerical Methods in Fluid Dynamics, 1980.

[126]Spalart, P. R. and Leonard, A., "Computation of Separated Flows by a Vortex-Tracing Algorithm," AIAA Paper 81-1246, June 1981.

[127]Spalart, P. R., Leonard, A., and Baganoff, D., "Numerical Simulation of Separated Flows," NASA TM 84328, Feb. 1983.

[128]Rao, B. M., Maskew, B., and Dvorak, F. A., "Theoretical Prediction of Dynamic Stall on Oscillating Airfoils," Paper presented at Annual National Forum of American Helicopter Society, May 1978.

[129]Maskew, B. and Dvorak, F. A., "Prediction of Dynamic Stall Characteristics Using Advanced Non-Linear Panel Methods," AFOSR TR 84-0975, April 1984.

[130]Mehta, U. B., "Dynamic Stall of an Oscillating Airfoil," AGARD CP 227, Sept. 1977.

[131]Shamroth, S. J. and Gibeling, H. J., "Analysis of Turbulent Flow about an Isolated Airfoil Using a Time-Dependent Navier-Stokes Procedure," AGARD CP 296, Sept. 1980.

[132]Sankar, N. L. and Tassa, Y., "Compressibility Effects on Dynamic Stall of an NACA 0012 Airfoil," *AIAA Journal*, Vol. 19, May 1981.

[133]Tassa, Y. and Sankar, N. L., "Dynamic Stall of NACA 0012 Airfoil in Turbulent Flow—Numerical Study," AIAA Paper 81-1289, June 1981.

[134]McCroskey, W. J., McAlister, K. W., Carr, L. W., and Pucci, S. L., "An Experimental Study of Dynamic Stall on Advanced Airfoil Sections," NASA TM 84245, July 1982.

[135]Costes, J. J., "Helicopter Rotor Aeroelastic Equilibrium Under Nonlinear Aerodynamic Forces," La Recherche Aerospatiale, No. 1982-5, 1982.

[136]Weissinger, J., "The Lift Distribution of Swept-Back Wings," NACA TM 1120, March 1947.

[137]DeYoung, J. and Harper, C. W., "Theoretical Symmetric Span Loading at Subsonic Speeds for Wings Having Arbitrary Plan Form," NACA Rept. 921, 1948.

[138]Brower, M., "Lifting Surface and Lifting Line Solutions for Rotor Blade Interaction with Curved and Straight Vortex Lines," Massachusetts Institute of Technology, Cambridge, ASRL TR 194-5, Nov. 1981.

[139]Kocurek, J. D., Berkowitz, L. F., and Harris, F. D., "Hover Performance Methodology at Bell Helicopter Textron," Paper presented at Annual National Forum of American Helicopter Society, May 1980.

[140]Van Dyke, M., "Lifting-Line Theory as a Singular-Perturbation Problem," Stanford University, Stanford, CA, Rept. SUDAER 165, Aug. 1963.

[141]Van Holten, T., "Computation of Aerodynamic Loads on Helicopter Rotor Blades in Forward Flight, Using the Method of the Acceleration Potential," Paper 74-54 presented at Ninth Congress of International Council of the Aeronautical Sciences, Aug. 1974.

[142]Van Holten, T., "The Computation of Aerodynamic Loads on Helicopter Blades in Forward Flight, Using the Method of the Acceleration Potential," Delft University of Technology, Delft, the Netherlands, Rept. VTH-189, March 1975.

[143]Van Holten, T., "On the Validity of Lifting Line Concepts in Rotor Analyses," *Vertica*, Vol. 1, No. 3, 1977.

[144]Cheng, H. K., "Lifting-Line Theory of Oblique Wings," *AIAA Journal*, Vol. 16, Nov. 1978.

[145]Cheng, H. K., "On Lifting-Line Theory in Unsteady Aerodynamics," *Proceeding of Symposium on Unsteady Aerodynamics*, edited by R. B. Kinney, Tucson, AZ, March 1975.

[146]Van Holten, T., "Some Notes on Unsteady Lifting-Line Theory," *Journal of Fluid Mechanics*, Vol. 77, No. 3, 1976.

[147]Ahmadi, A. R., "An Asymptotic Unsteady Lifting Line Theory with Energetics and Optimum Motion of Thrust-Producing Surfaces," Massachusetts Institute of Technology, Cambridge, FDRL Rept. 80-2, Sept. 1980.

[148]Guiraud, J.-P. and Slama, G., "Lifting Line Asymptotic Theory in Incompressible Oscillating Flow," La Recherche Aerospatiale, No. 1981-1, Jan.-Feb. 1981.

[149]Piziali, R. A., "Method for the Solution of the Aeroelastic Response Problem for Rotary Wings," *Journal of Sound and Vibration*, Vol. 4, No. 3, 1966.

[150]Miller, R. H., "Unsteady Air Loads on Helicopter Rotor Blades," *Journal of the Royal Aeronautical Society*, Vol. 68, No. 640, April 1964.

[151]Cook, L. P. and Cole, J. D., "Lifting Line Theory for Transonic Flow," *SIAM Journal on Applied Mathematics*, Vol. 35, No. 2, Sept. 1978.

[152]Cook, L. P., "Lifting-Line Theory for a Swept Wing at Transonic Speeds," *Quarterly Journal of Mechanics and Applied Mathematics*, Vol. 37, No. 2, July 1979.

[153]Cheng, H. K. and Meng, S. Y., "Lifting Line Theory of Oblique Wings in Transonic Flows," *AIAA Journal*, Vol. 17, Jan. 1979.

[154]Cheng, H. K. and Meng, S. Y., "The Oblique Wing as a Lifting-Line Problem in Transonic Flow," *Journal of Fluid Mechanics*, Vol. 97, No. 3, 1980.

[155]Cheng, H. K., Meng, S. Y., Chow, R., and Smith, R. C., "Transonic Swept Wings Studied by the Lifting Line Theory," *AIAA Journal*, Vol. 19, Aug. 1981.

[156]Vaidyanathan, A. R. and Pierce, G. A., "Evaluation of an Asymptotic Method for Helicopter Rotor Airloads," Paper presented at Annual National Forum of American Helicopter Society, May 1983.

[157]Vaidyanathan, A. R. and Pierce, G. A., "A Discretized Asymptotic Method for Unsteady Helicopter Rotor Airloads," AIAA Paper 83-0989, May 1983.

[158]Caradonna, F. X. and Tung, C., "A Review of Current Finite Difference Rotor Flow Methods," Paper presented at Annual National Forum of American Helicopter Society, June 1986.

[159]Srinivasan, G. R. and McCroskey, W. J., "Numerical Simulations of Unsteady Airfoil—Vortex Interactions." *Vertica*, Vol. 10, No. 4, 1986.